Micro-modification of glass by femtosecond laser—fundamentals and applications

Jianrong Qiu

South China University of Technology

Ac

Res

Pro

(Kyoto University, Japan)

Prof. P. K

Profs. C. … *Zeng, My*

students a

"Imagination is more important than knowledge"

Albert Einstein

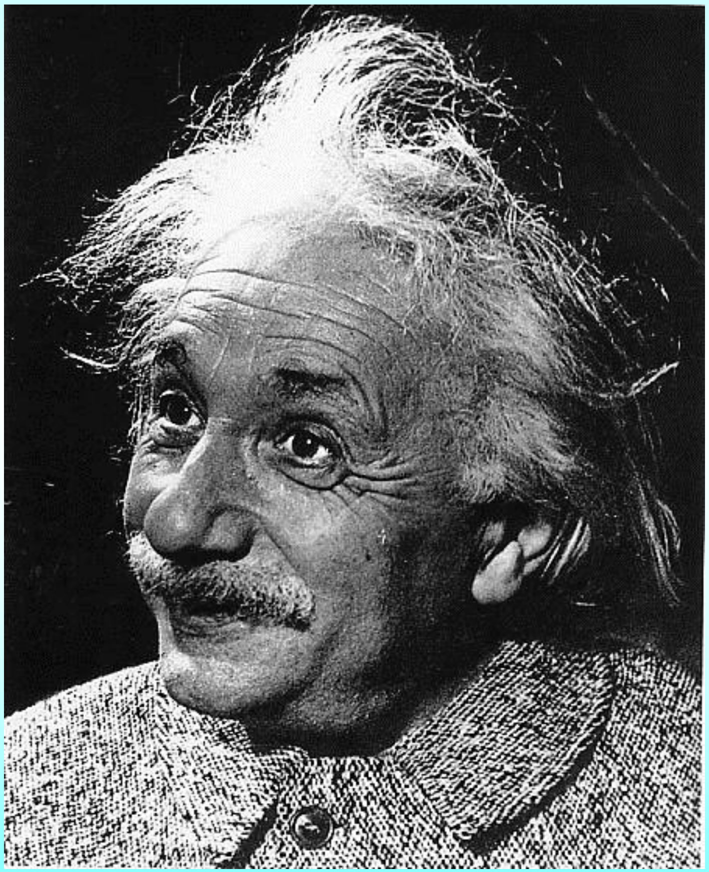

1 $\varepsilon = h\nu$

2 $\varepsilon = mc^2$

3 $P = h/\nu$

4 $\rho = dN/d\tau$

Outline

1、Fundamentals of light-matter interaction

2、Femtosecond laser induced phenomena in glass

3、Femtosecond laser induced microstructures in glass

4、Conclusions

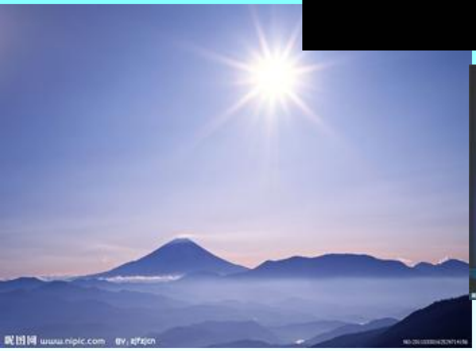

Natural light Bonfire Electric light Laser

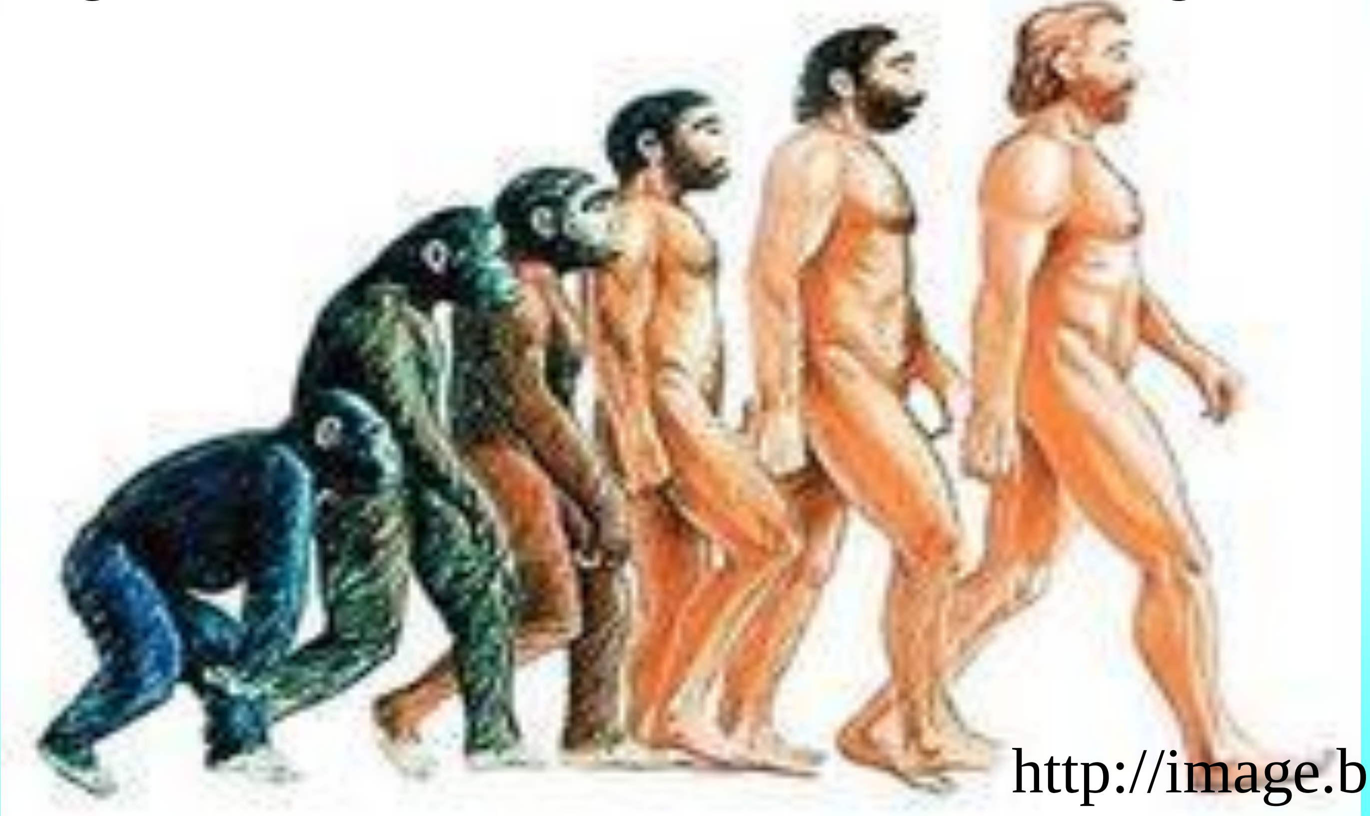

http://image.baidu.com/

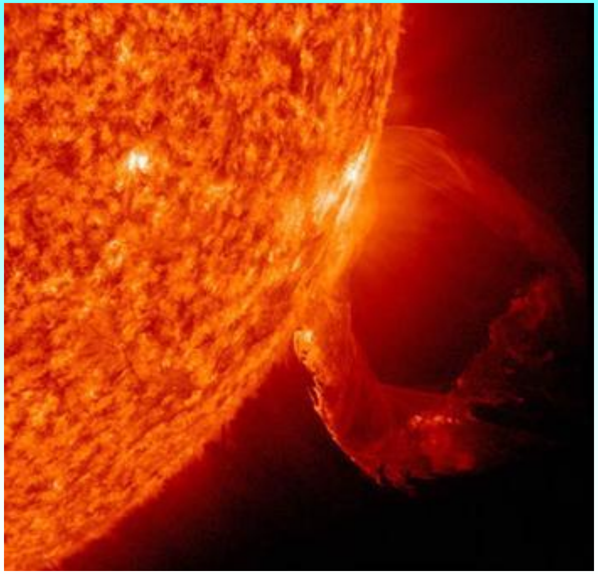

Sun

Nuclear explosion

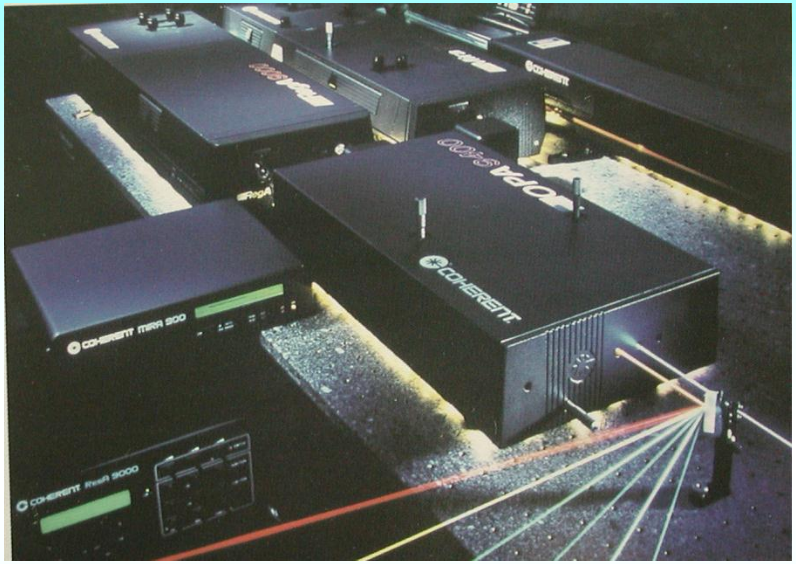

Ti:Sapphire femtosecond laser system (Coherent Co. Ltd)

($>2x10^{16}W/cm^2$)

Features of laser

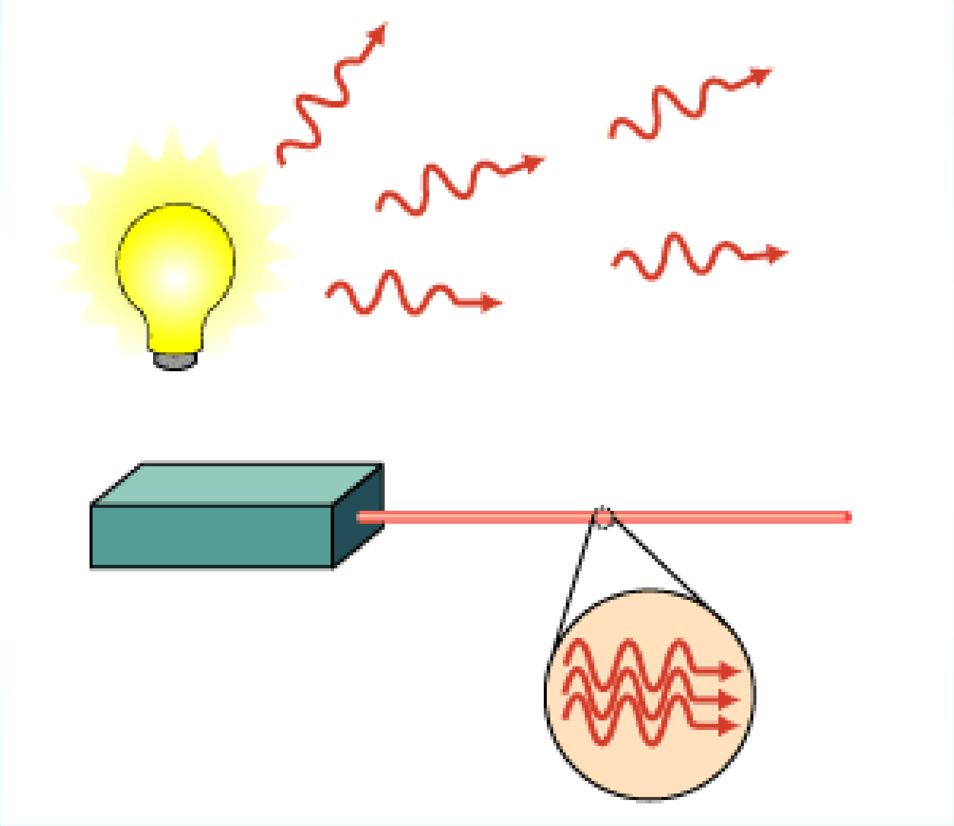

Monochromatic (10^{-8}nm)， **Narrow beam divergence(38000km/1km)**

High brightness ($4x10^{13}$cd/m^2, $1.7x10^9$cd/m^2(sun))

Coherent

Features of femtosecond laser

$1fs=10^{-15}s$

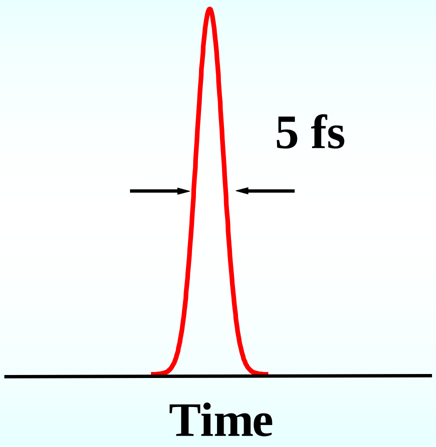

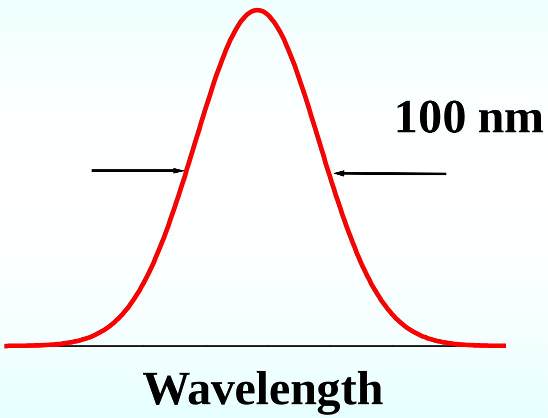

1) ultrashort pulse
2) ultrahigh electric field (>$2x10^{16}W/cm^2$)
3) ultrabroad bandwidth (coherent) ($\Delta\nu = k / \Delta\tau$)

Characteristic time of ultrafast processes

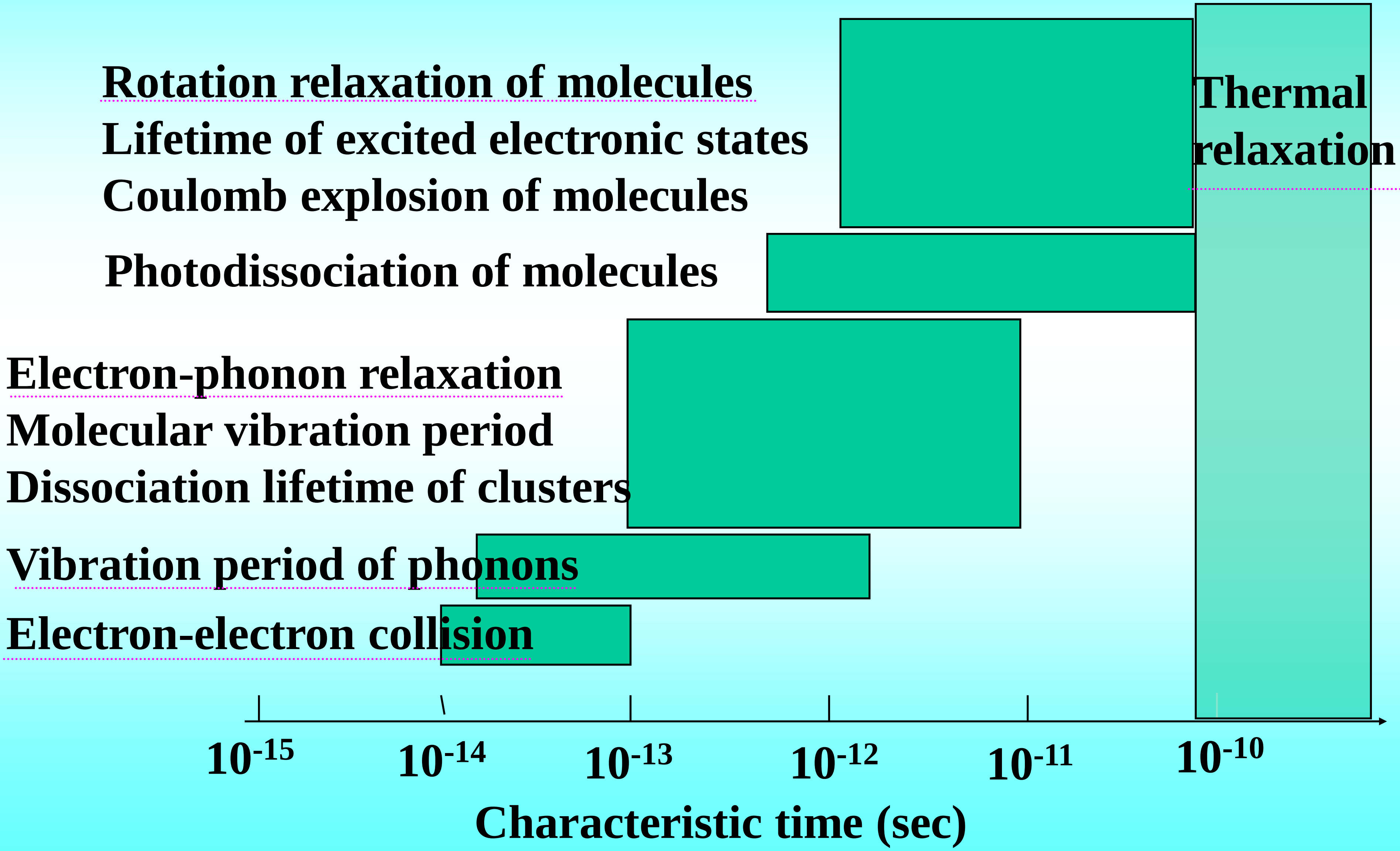

Laser-matter interactions

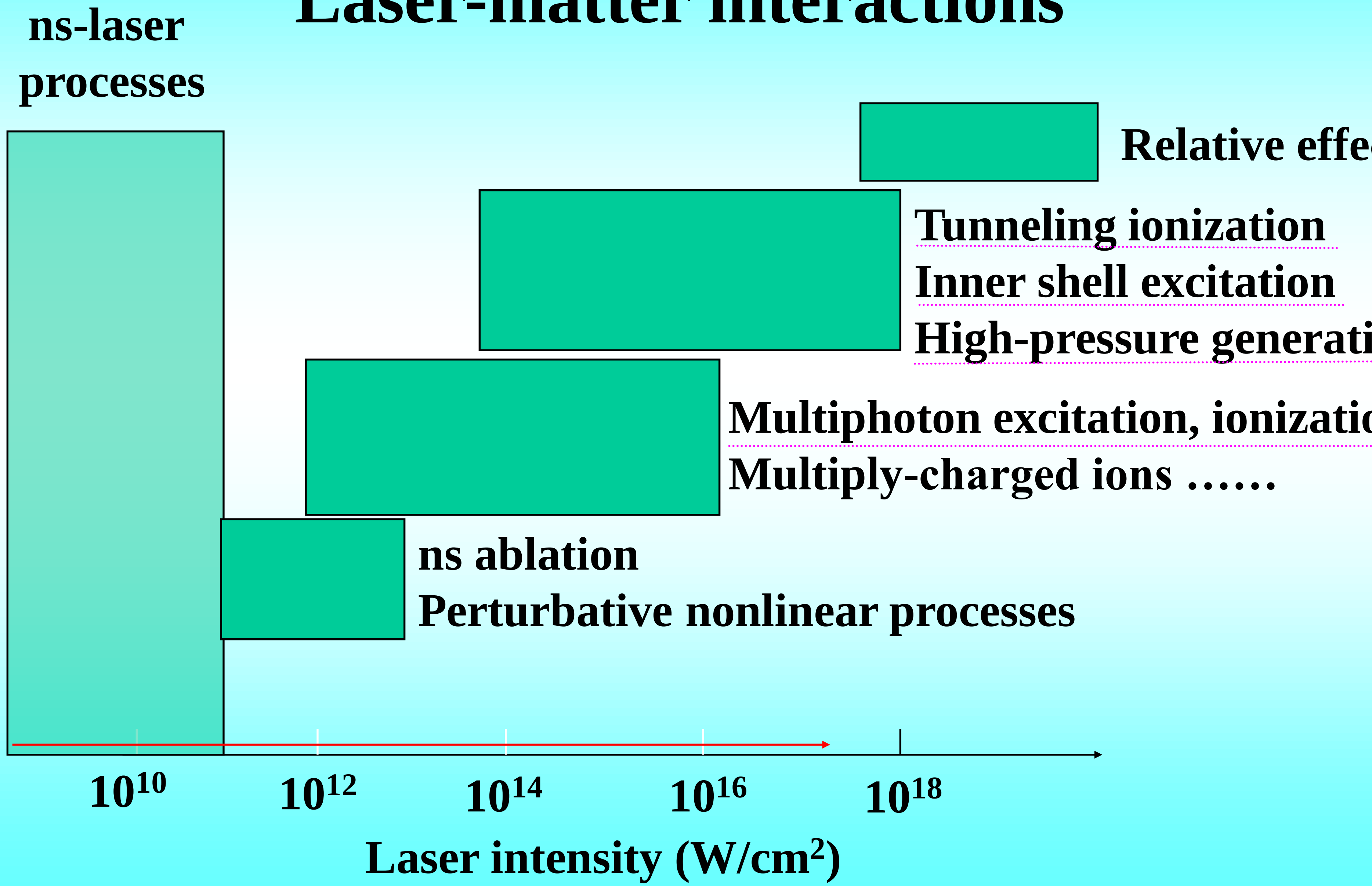

Characteristics of fs laser with matter：

1) Elimination of the thermal effect due to extremely short energy deposition time

2) Participation of various nonlinear processes enabled by high localization of laser photons in both time and spatial domains

3) Broadband spectrum (($\Delta \nu = k / \Delta \tau$)
Pulse modulation

3-dimensional micro-modification

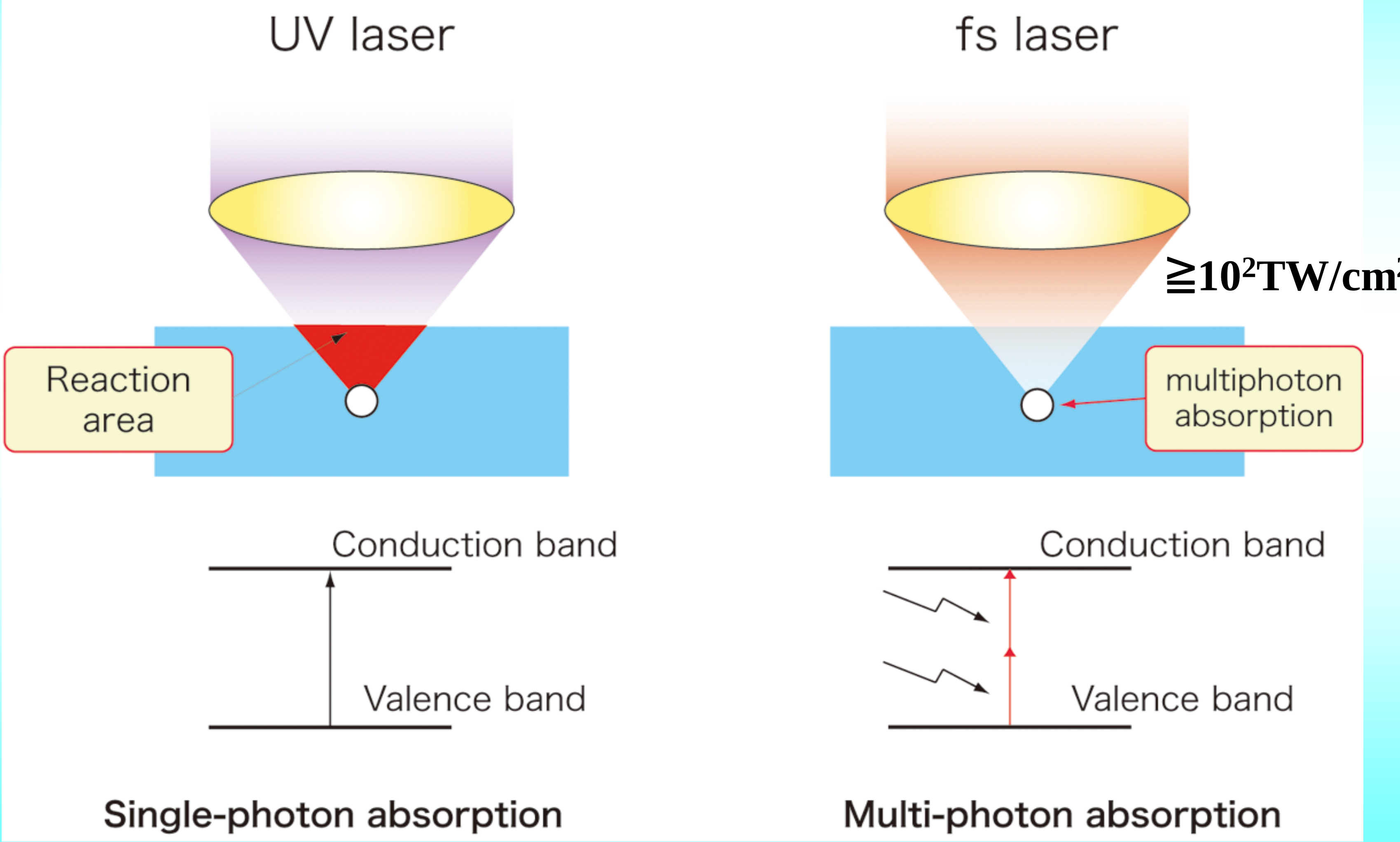

$$\chi = \sigma \left(I/h\nu \right)^{n}$$

Optical setup for manipulating glass structure

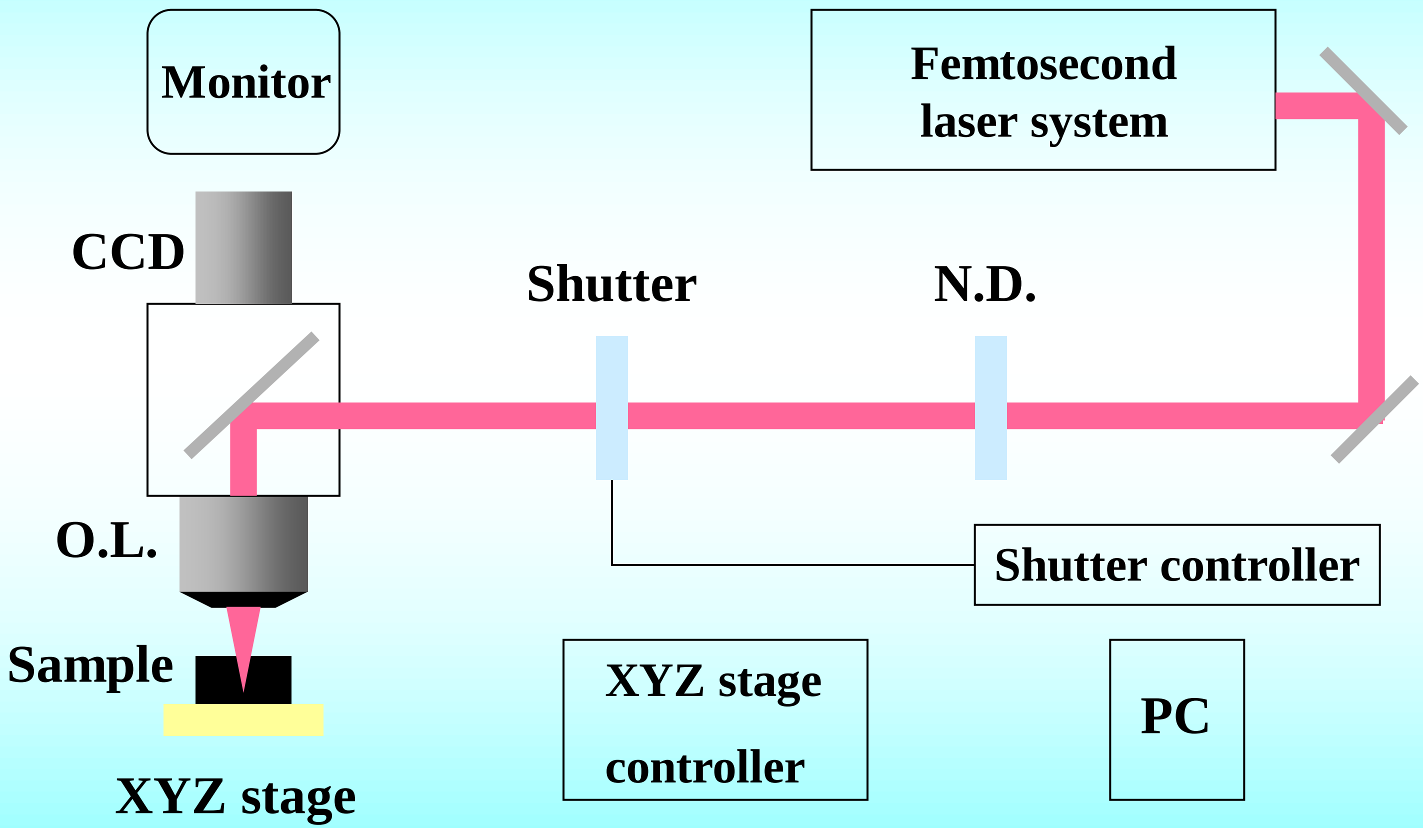

Controlling parameters：

1) Fs laser
   Pulse energy, Pulse width, Pulse repetition rate,
   Polarization, Pulse Phase, Pulse front tilt, Pulse train…

2) Focusing system
   NA of lens, immersion oil

3) Controlling system
   Irradiation time, Scanning direction, Scanning speed,
   Scanning time

Properties of glass：

Amorphous structure、glass transition

Isotropic, Designable composition and micro-structure

Transparent and homogenous

Metastable

Solid solvent

Composition controllable

Easy fabrication

Easy processing

Multi-processing PS, Cryst. Ion Change.

Fs laser induced phenomena

Transient phenomena

Permanent phenomena

Various emissions during fs laser irradiation

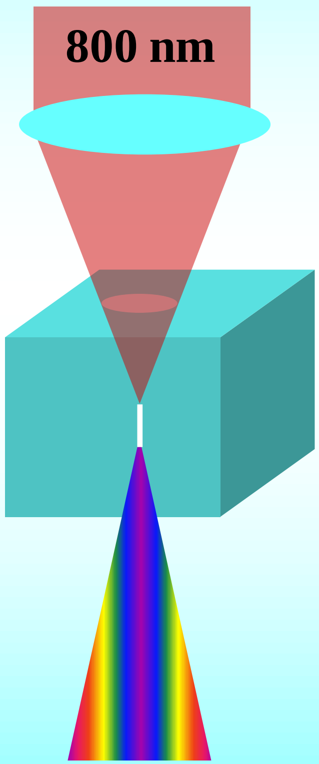

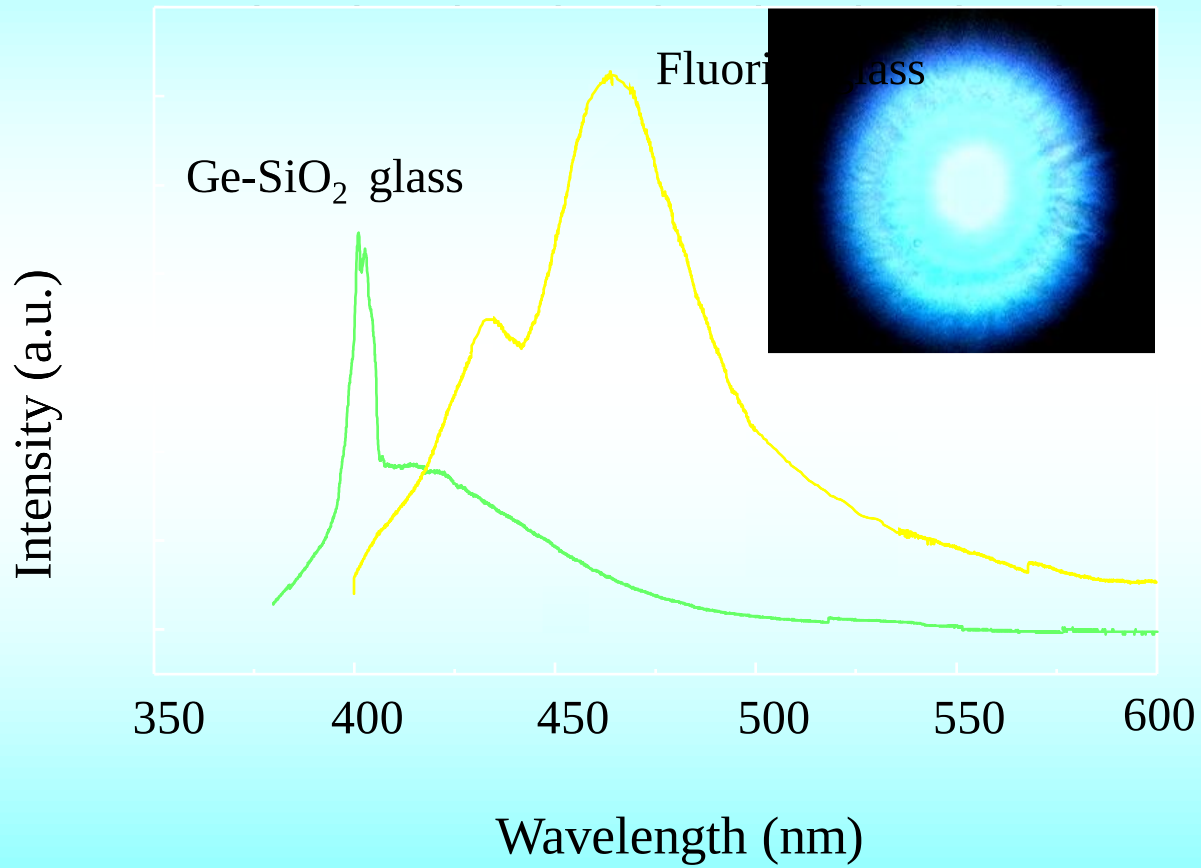

Typical emission spectra of fluoride glass and Ge-doped silica glass during irradiation of a ultrashort-pulse laser. Wavelength, average power and pulse width of the laser were 800 nm 200 mW and 120 fs at 200 kHz, respectively.

Fs laser induced long lasting phosphorescence

欠陥があるゆえに発光する　Emitting only with defects

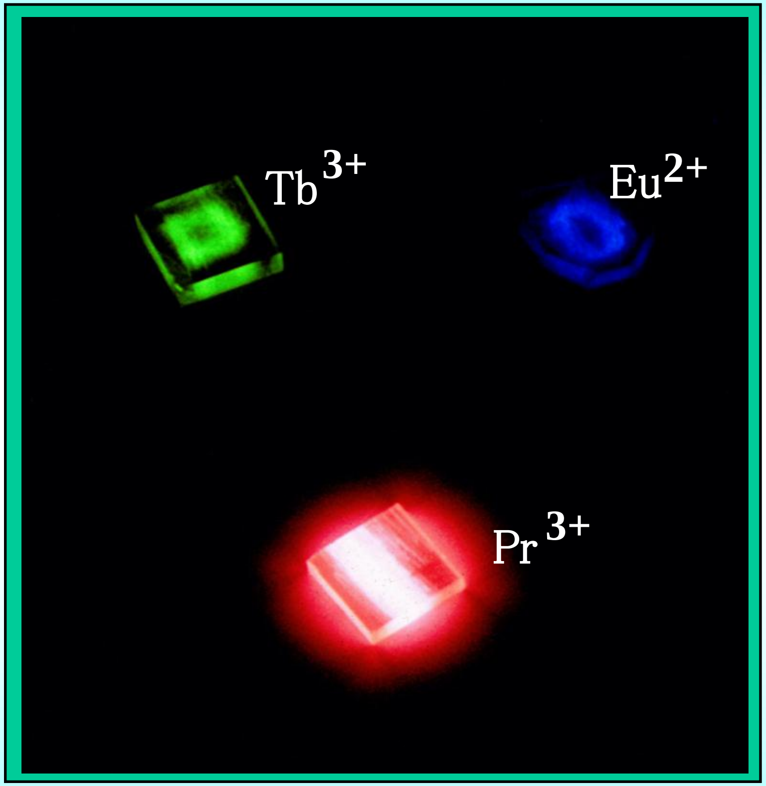

Emission states of phosphorescence in rare-earth-doped fluorozirconate glasses induced by femtosecond laser

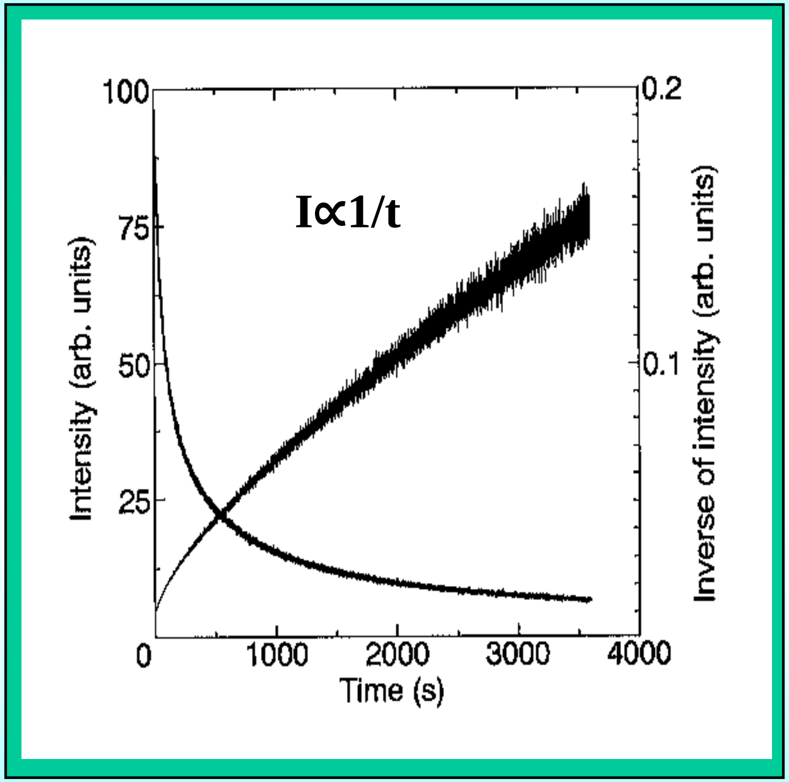

Decay curve of the phosphorescence at 543nm in the femtosecond laser irradiated Tb^{3+} -doped fluorozirconate glass

Appl. Phys. Lett., 75(1998)1940.

FS laser-induced polarization-dependent emission

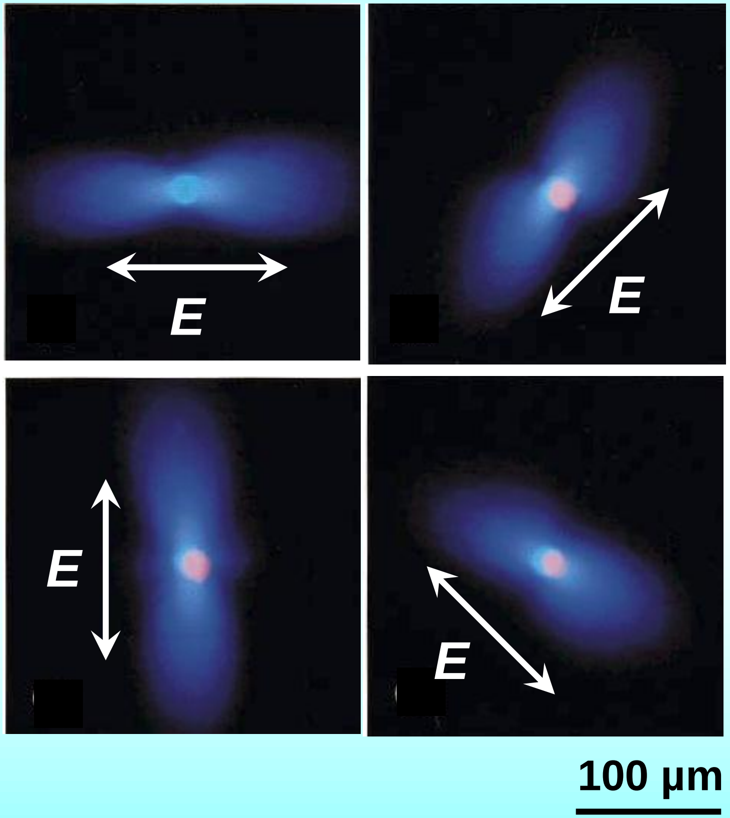

Ge-SiO_2

Phys. Rev. Lett., 82(1999)2199.

Memorized polarization-dependent emission

Appl. Phys. Lett., 77(2000)1940.

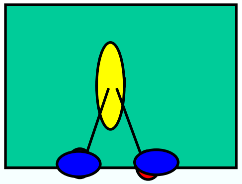

10X(NA=0.30), 200mW, 150fs, 200kHz, 4mm

Eu-doped AlF_3-based glass

a: 0min   b: 5min   c:10min   d: 20min

Single fs laser beam-induced polarization-dependent nanograting

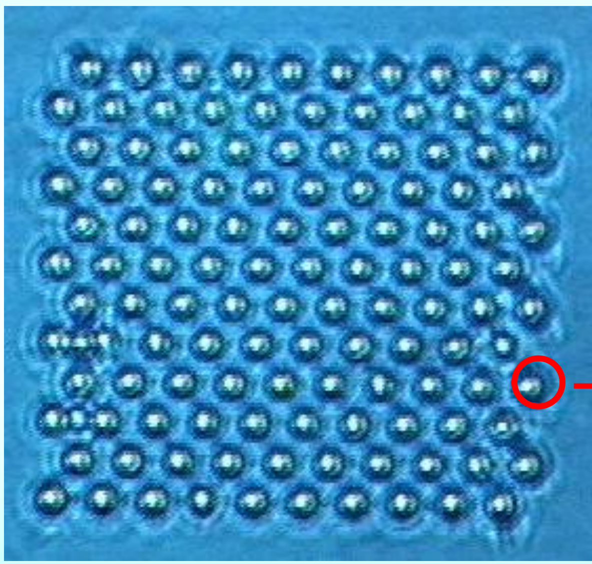

100× (0.95)
120fs
200kHz
200mW
1s

SiO_2

Optical microphotograph

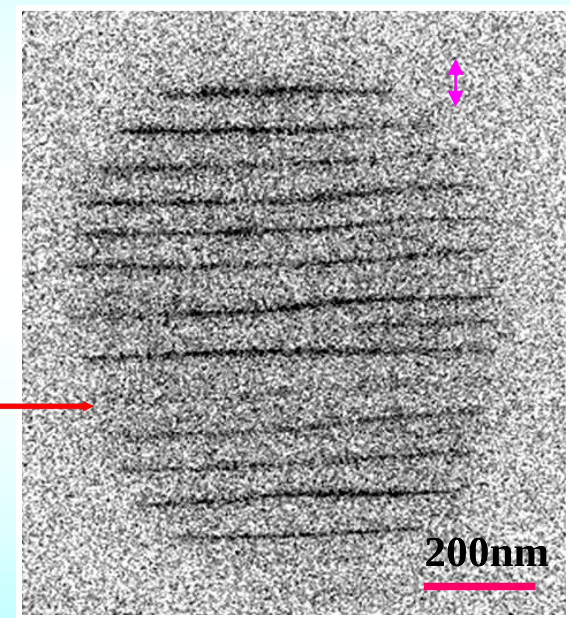

BEI image of SEM

Phys. Rev. Lett., 91(2003)247405.

Single fs laser beam-induced polarization-dependent nanograting

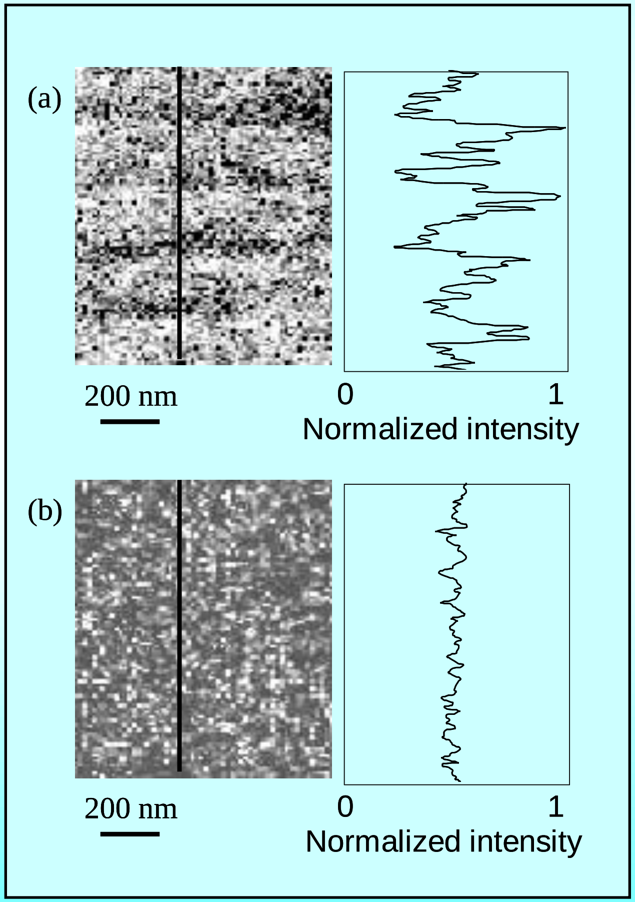

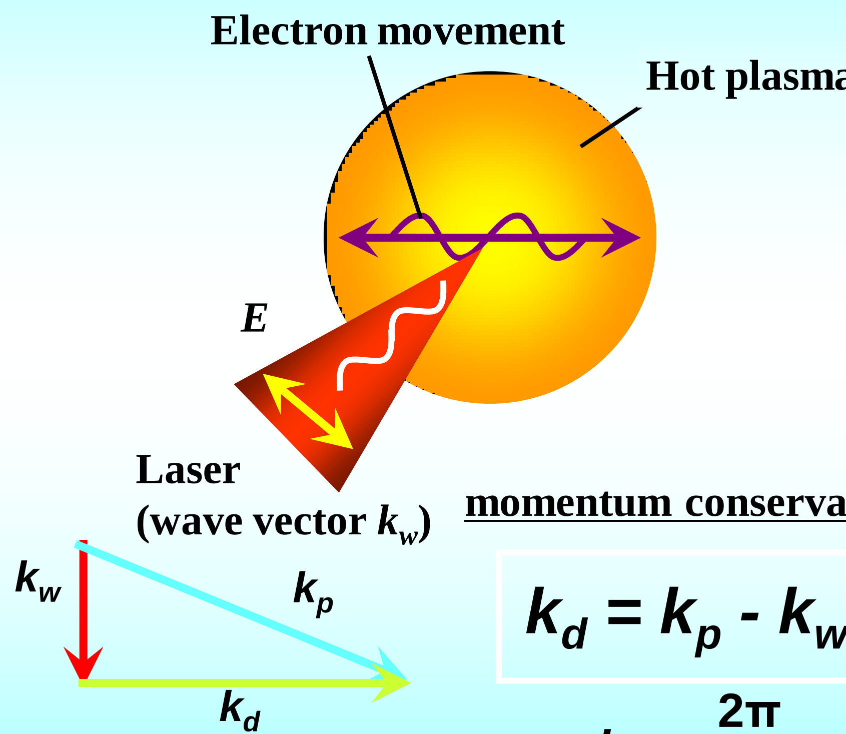

momentum conservation

$$k_d = k_p - k_w$$

$$k_d = \frac{2\pi}{\Lambda}$$

k_w: laser wave vector

k_p: plasmon wave vector

k_d: dielectric constant modulation vector

Λ: period of nanostructure

O and Si concentration AES mapping

Mechanism of the nanograting

5D optical memory using fs laser induced birefringence

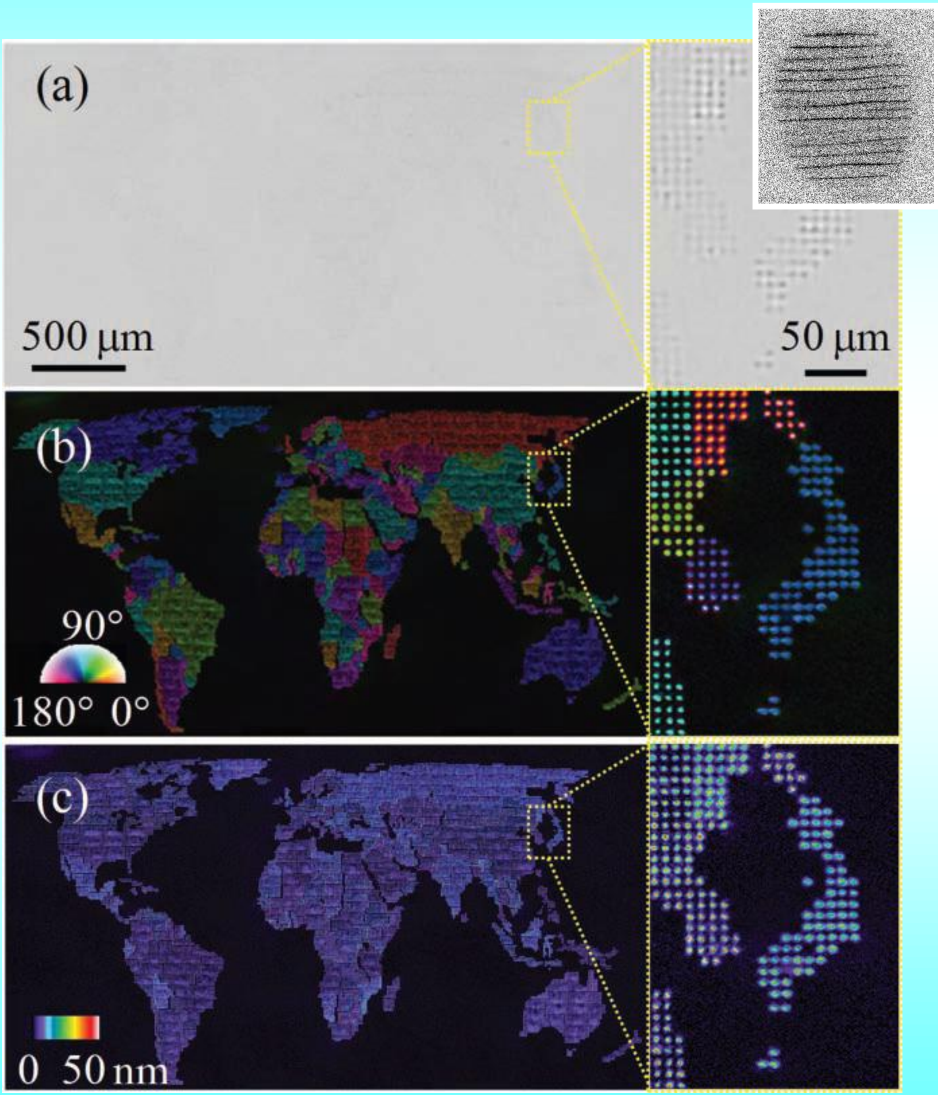

***Adv. Mat.*, 24(2010)1-5.**

Images of the “ *Small World Map* ” taken with optical (a) and polarization (b – azimuth angle, c – retardance) microscopes. The structure was printed in silica glass using femtosecond laser beam modulated with LCOS-SLM. Actual size of the structure is 3.4 mm × 1.8 mm. The highly magnified images of the marked area are shown on the right.

Single femtosecond laser beam-induced rotated nanograting

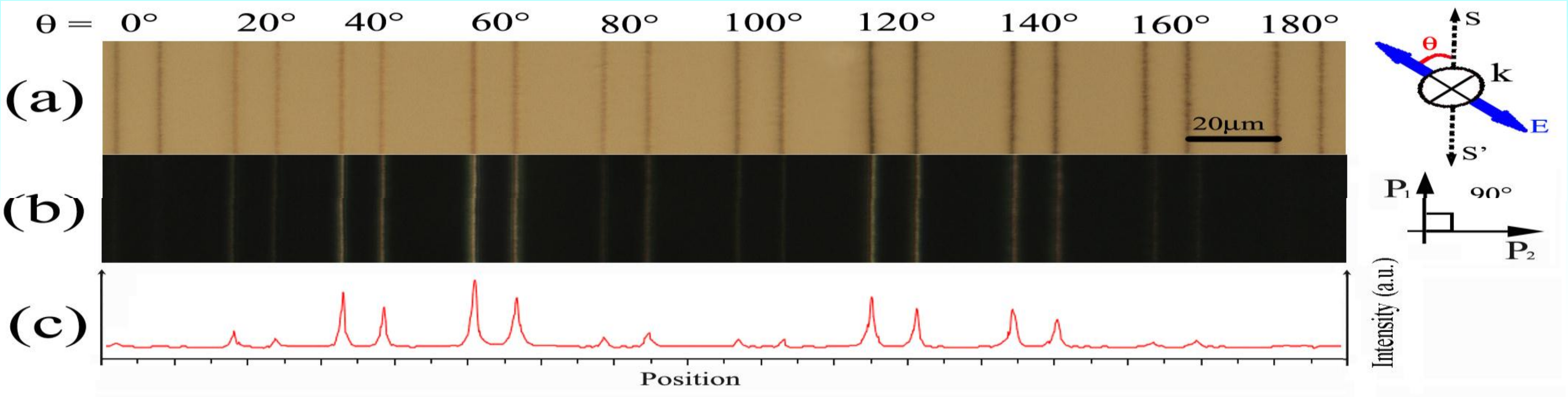

200kHz

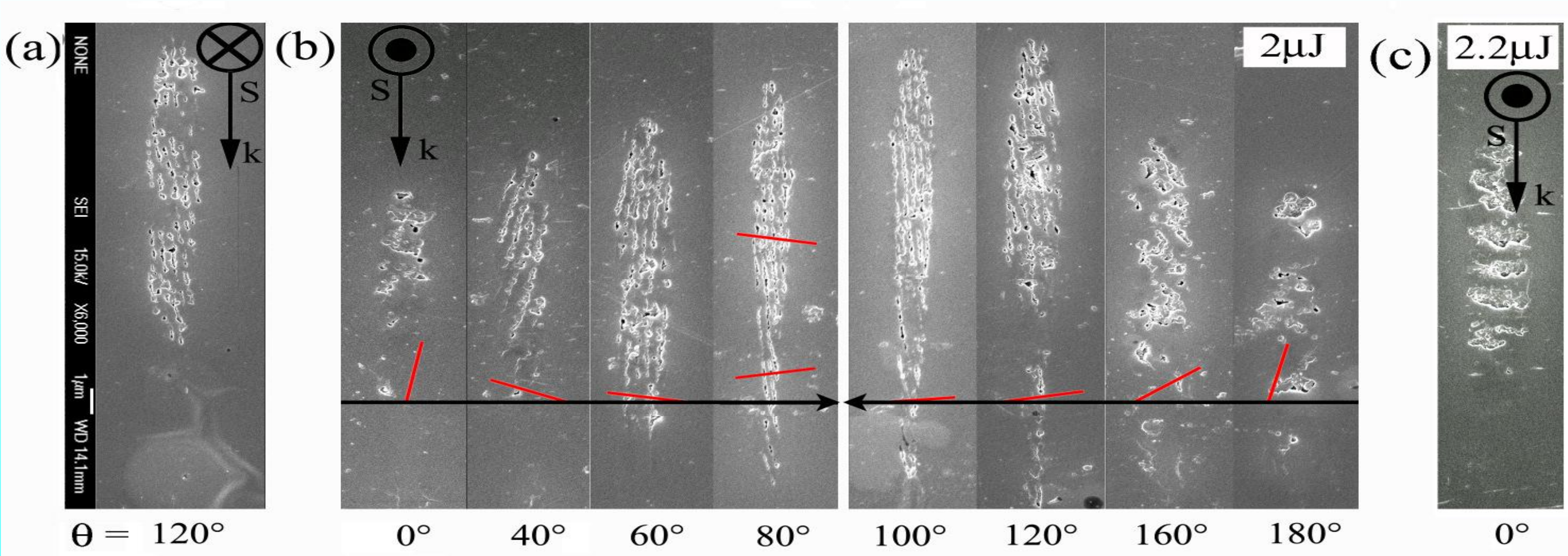

Single femtosecond laser beam-induced rotated nanograting

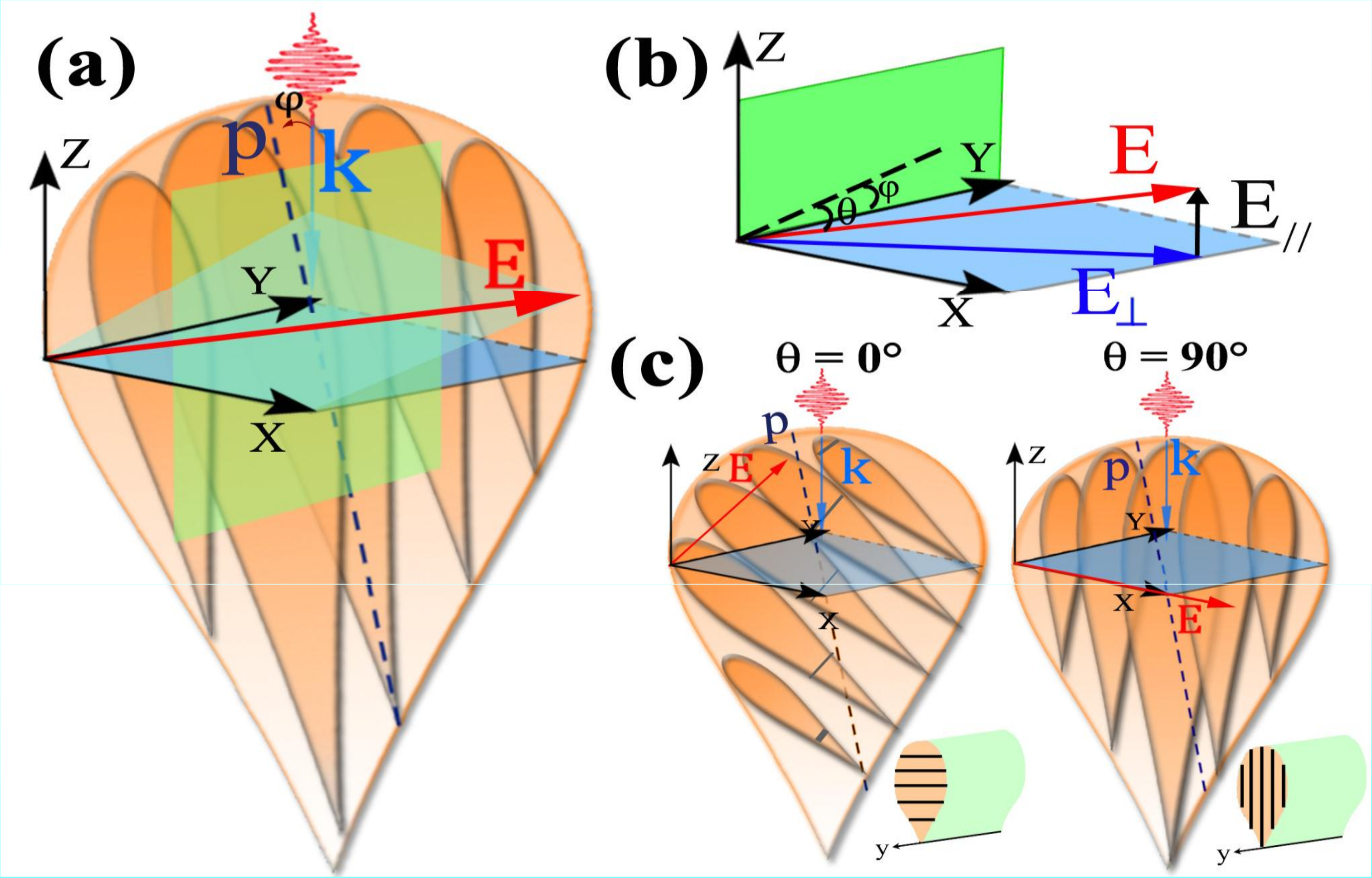

Fs laser-induced nano-void array

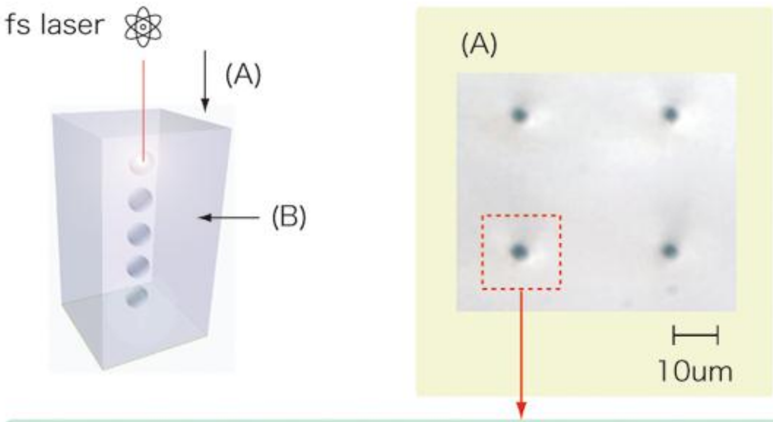

Condition :

Repetition rate : 1kHz
Pulse number : 250 pulses
Pulse energy : 10 uJ
Objectve lens : 100× (NA = 0.9)

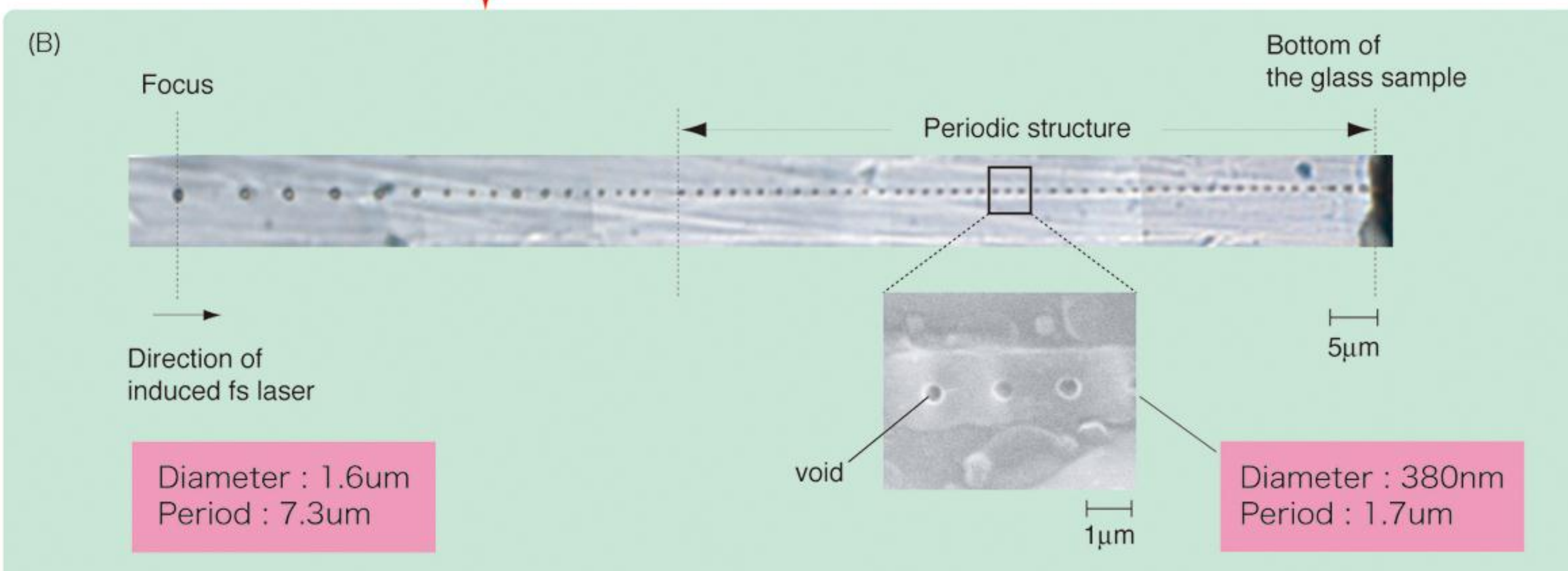

Nano Lett., **5(2005)1591.**

Non-paraxial nonlinear Schrodinger equation to exactly describe the pulse propagation:

$$\frac{\partial^2 E}{\partial z^2} + i2k\frac{\partial E}{\partial z} + \nabla_\perp E = kk''\frac{\partial^2 E}{\partial \xi^2} \underbrace{- ik\sigma(1 + i\omega\tau_c)\rho E - ik\beta^{(K)}|E|^{2K-2}E - 2kk_0 n_2 |E|^2 E}_{\text{Nonlinear effects}} \qquad (1)$$

Electron density

$$\frac{\partial \rho}{\partial \xi} = \frac{1}{n^2}\frac{\sigma}{E_g}\rho|E|^2 + \frac{\beta^{(K)}|E|^{(2K)}}{K\hbar\omega} - \frac{\rho}{\tau_r}$$

Analysis of interface spherical aberration by P. Török et al (electromagnetic diffraction th

$$I_0^{(e)} = \int_0^{\phi_{max}} (\cos\phi_1)^{1/2}(\sin\phi_1)\exp\left[ik_0\underbrace{\psi(\phi_1,\phi_2,-d)}_{\text{aberration function}}\right]\times(\tau_s + \tau_p\cos\phi_2)J_0(k_1 r_p \sin\phi_p \sin\phi_1)\times\exp(ik_2 r_p\cos\phi_p\cos\phi_2)\,d\phi_1 \qquad (3)$$

Appl. Phys. Lett., **92(2008)121113**

Fs laser-induced nano-void array

Self-aligned voids structure

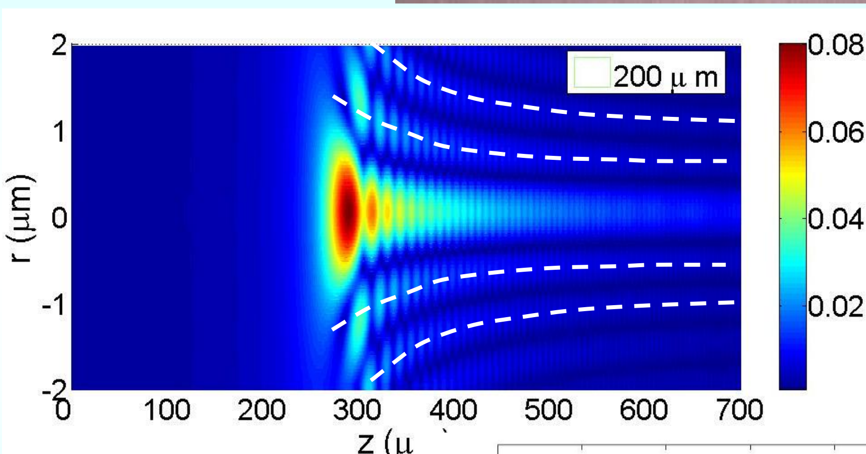

Appl. Phys. Lett.**,**

92(2008)92904.

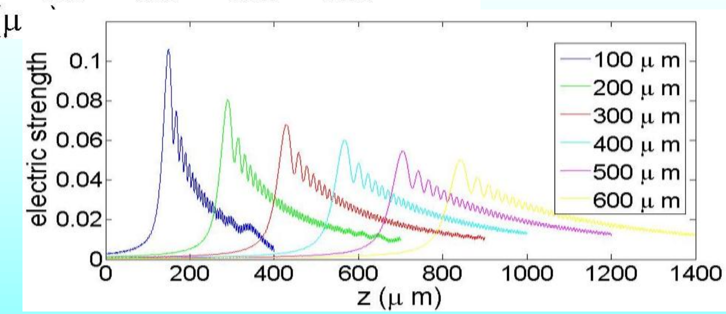

electromagnetic diffraction theory

On-axis electric strength distribution along the direction of the laser propagation (spherical aberration)

Fs laser-induced nano-void array

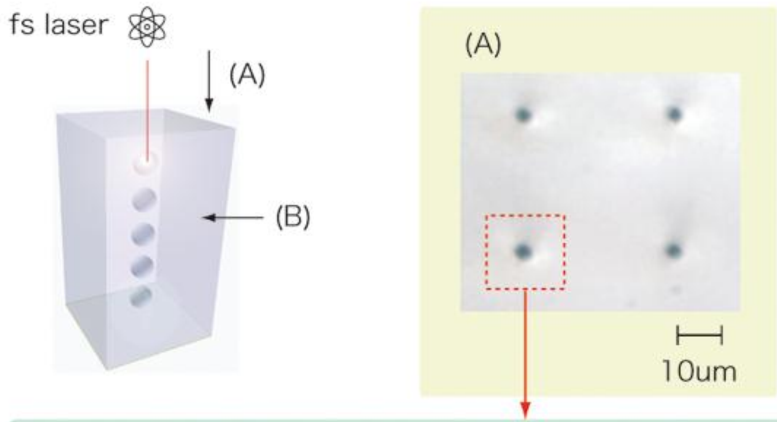

Condition :

Repetition rate : 1kHz
Pulse number : 250 pulses
Pulse energy : 10 uJ
Objectve lens : 100× (NA = 0.9)

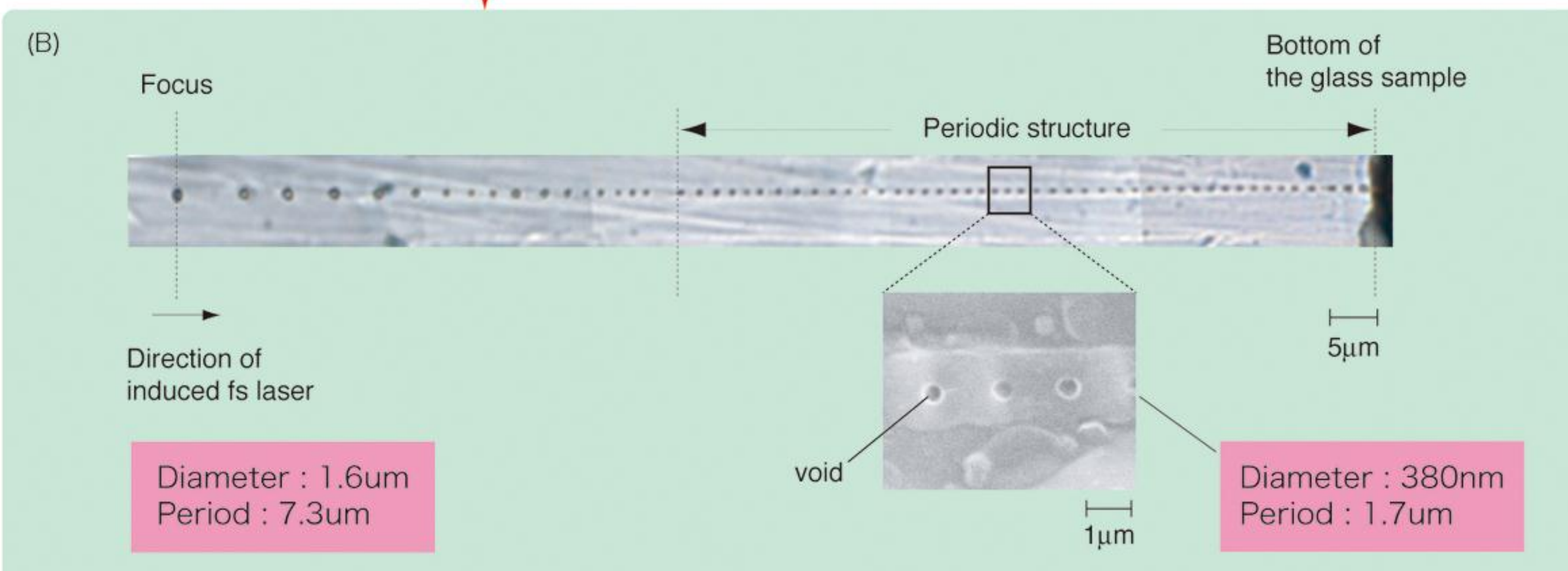

Nano Lett., **5(2005)1591.**

Fs laser-induced tilted grating

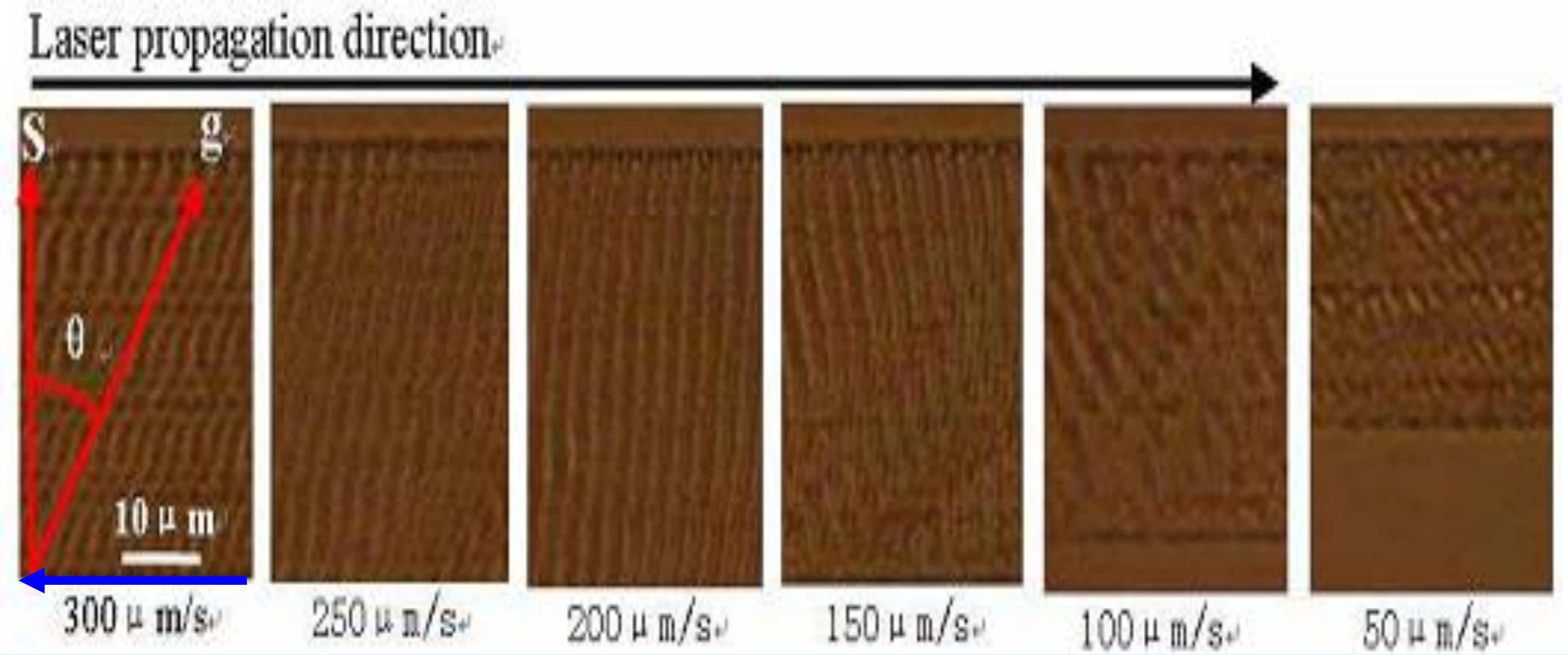

***Appl. Phys. Lett.*, 101(2007)23112.**

Fs laser induced migration of ions

$65SiO_2$-$10CaO$-$20Na_2O$-$5Eu_2O_3$

***Opt. Lett.*, 92(2009)141112.**

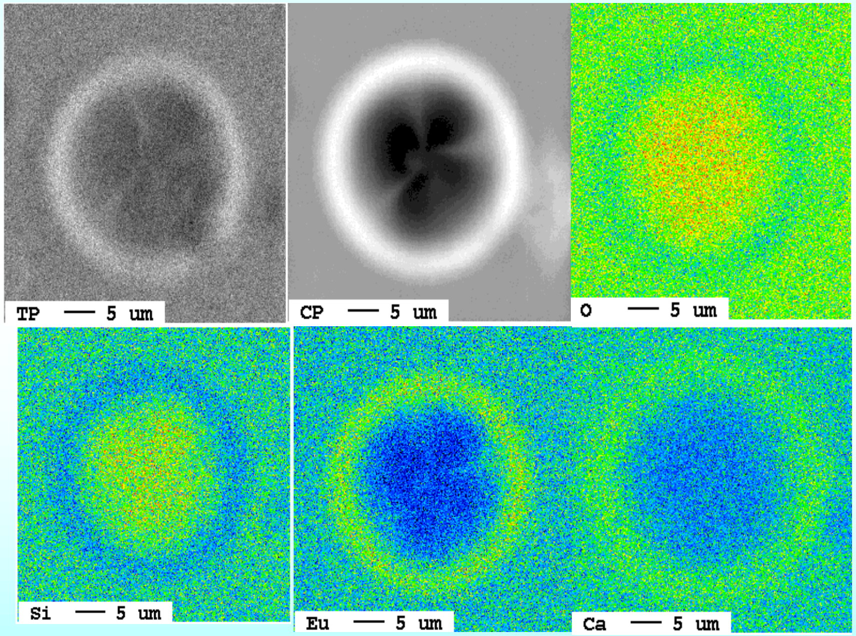

EPMA mapping showing element distribution from the laser focal point to the edge of the laser modified zone.

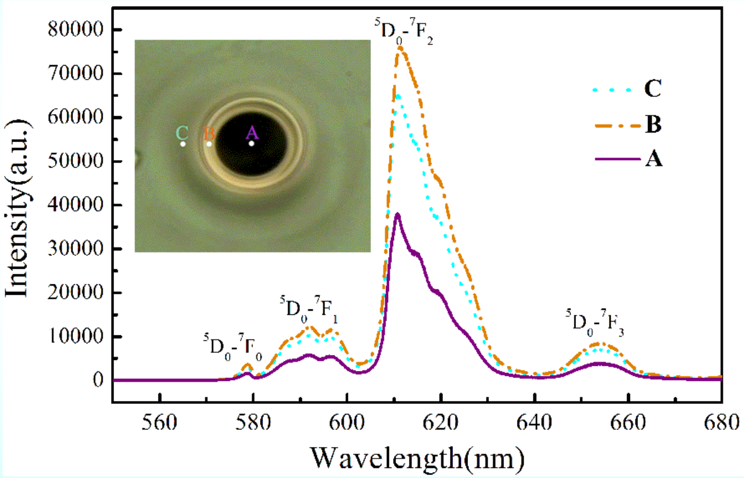

Confocal fluorescence spectra from different positions(A-C) of a laser modified zone.

Fs laser induced migration of ions

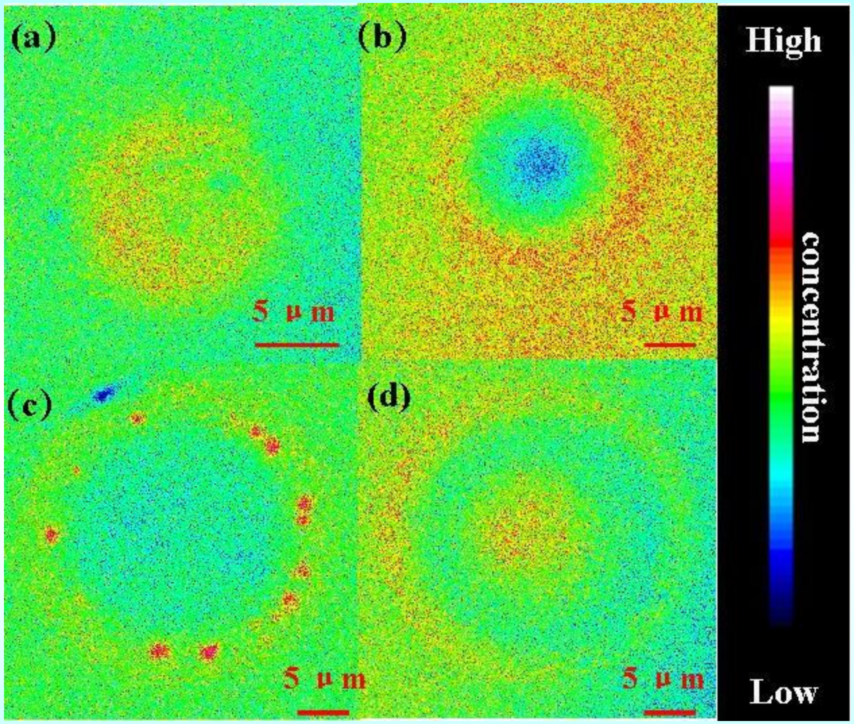

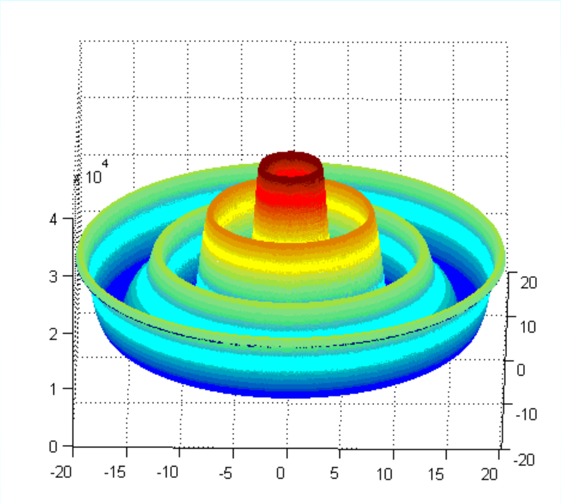

simulation

(Color online) EPMA mapping showing the distribution of Ca^{2+} ions in the glass with different pluse energies. (a) 2μJ, (b) 2.72μJ, (c) 3.12μJ, (d) 3.52μJ

Micro structures looks like bear-paw induced by fs laser beam

J. Appl. Phys., 106(2009)121113.

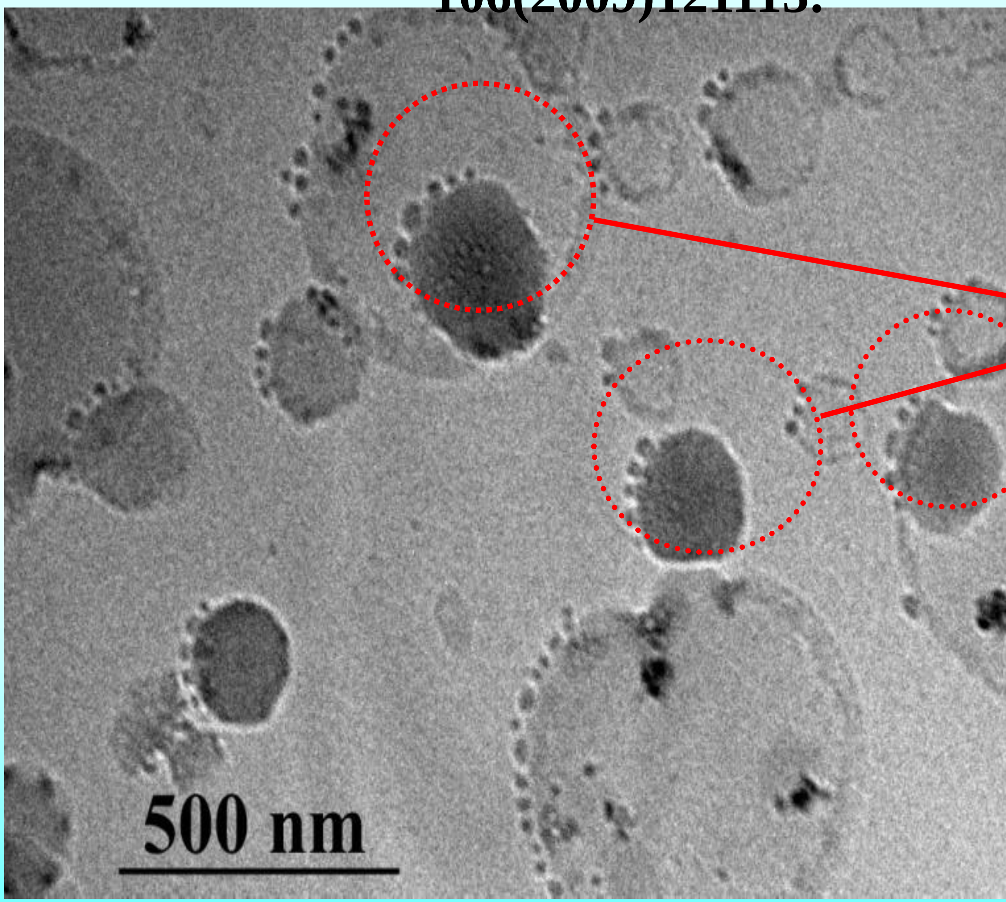

Na$_2$O-CaO-SiO$_2$ glass

Famous Chinese Dish
Bear-paw
（熊掌）

Fs laser induced mysterious structure

Opt. Express, 2012

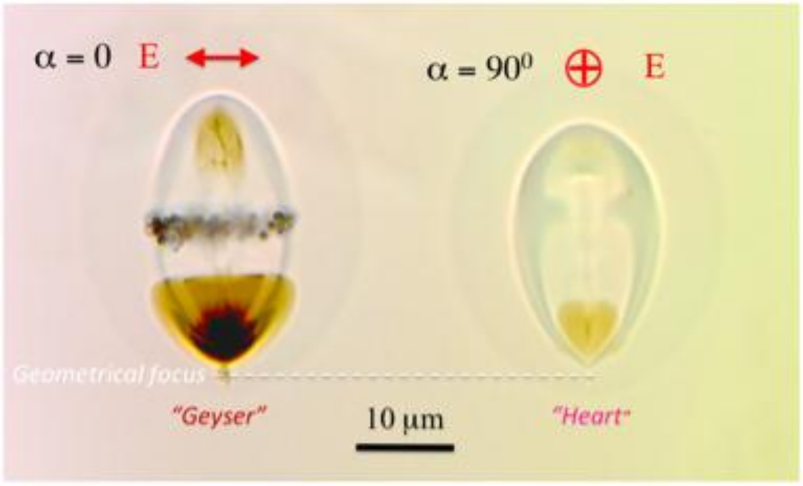

Aluminosilicate glass
250KHz
120fs

Femtosecond laser induced microstructures

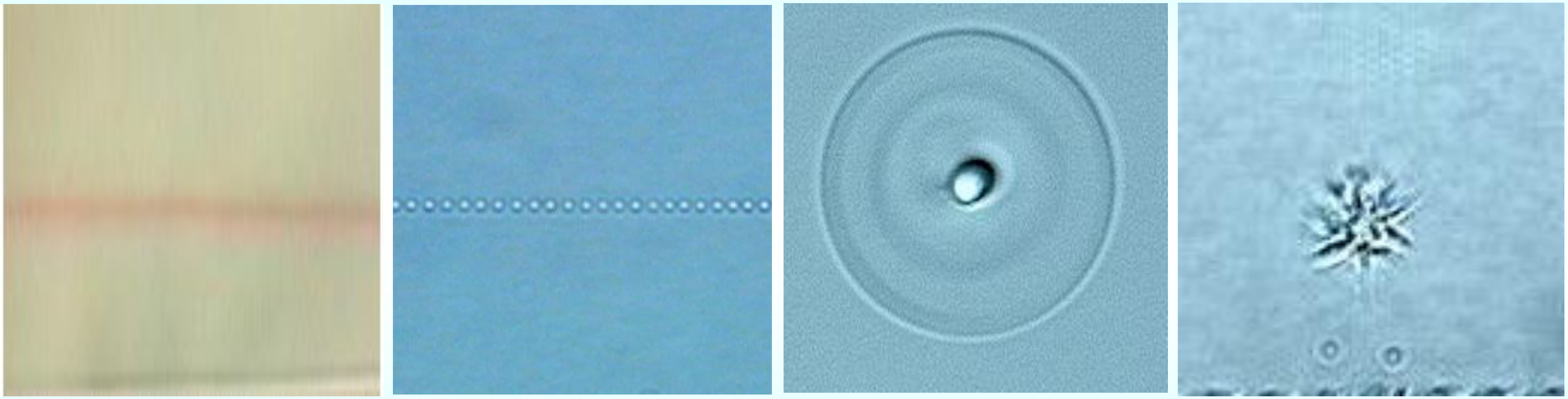

Various structures induced by 800 nm, 120fs laser-pulses

The Chemical Record, **109(2005)25.**

Fs laser induced valence state change of transition metal ions

$Mn^{2+} + Fe^{3+} + \rightarrow Mn^{3+} + Fe^{2+}$

1KHz
10x(NA=0.3)
3mW
120fs

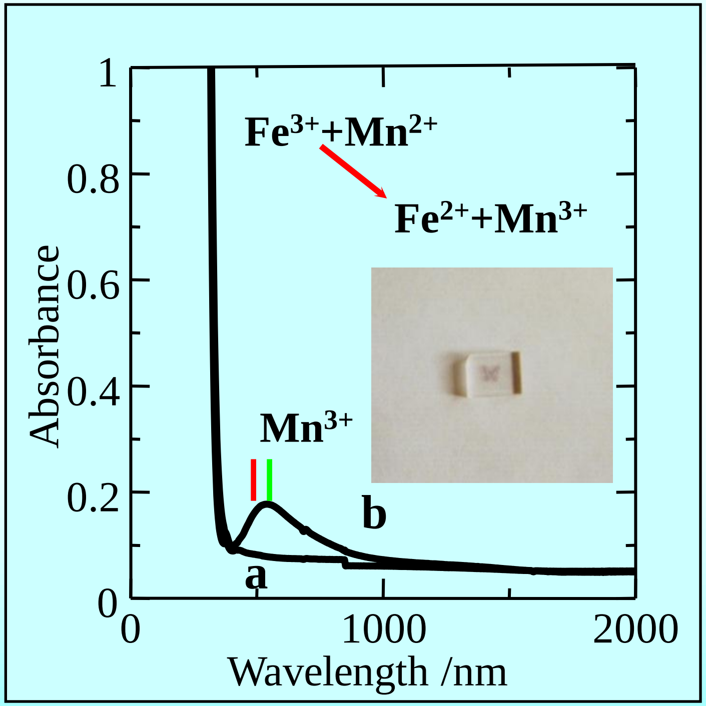

20Na$_2$O-10CaO-70SiO$_2$-0.1Fe$_2$O$_3$-0.1MnO (mol%)

Absorption spectra
a: before irradiation b: after irradiation (iron and manganese)

Appl. Phys. Lett., 79(2001)3567.

Fs laser induced valence state change of **noble metal ions**

$Ag^{+} \rightarrow Ag^{2+} + Ag$

***Opt. Express*, 12(2004)4035.**

Na_2O-Al_2O_3-P_2O_5-$0.1Ag_2O$ (mol%)

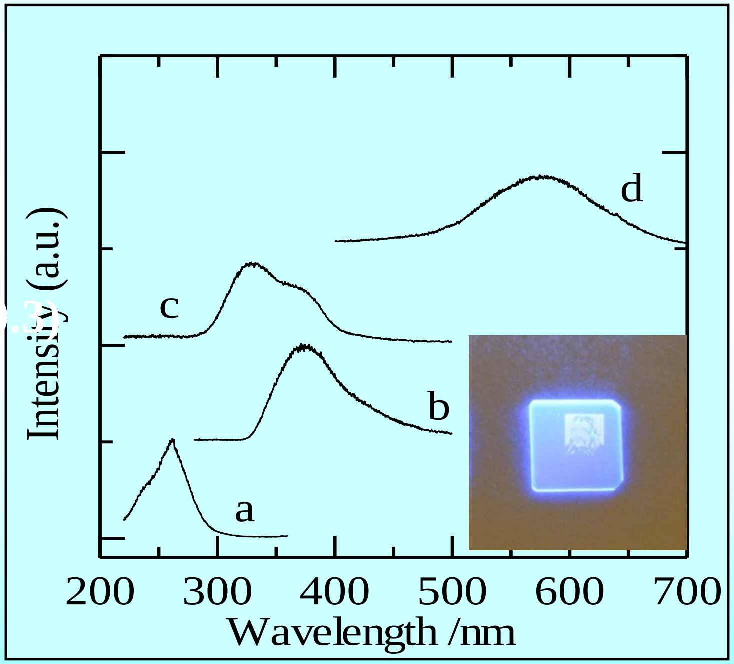

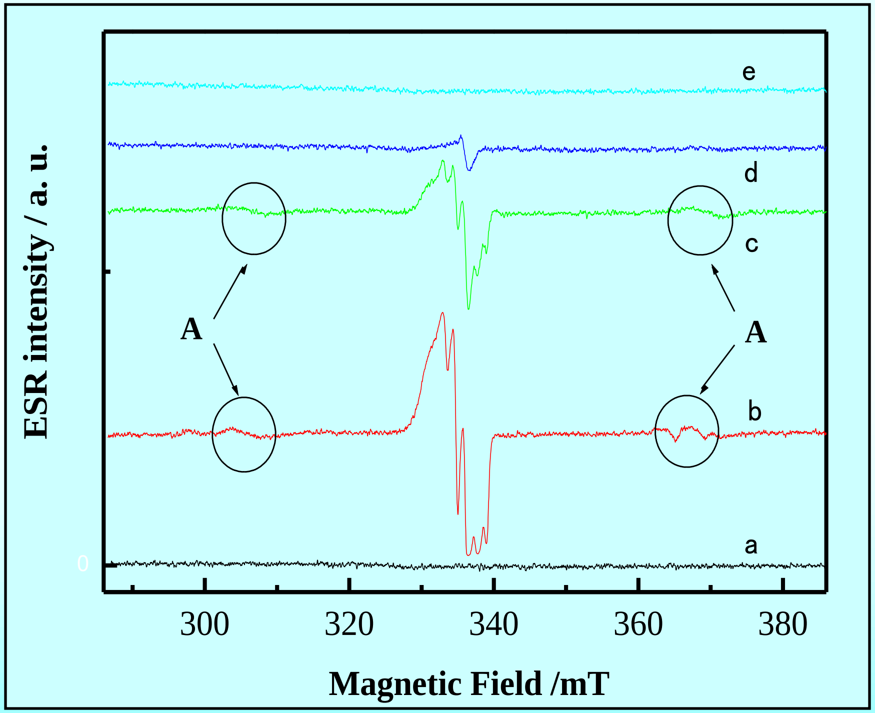

Emission and excitation spectra
a, b: before irradiation
c, d: after irradiation

ESR spectra
a: before irradiation b: after irradiation

Fs laser induced valence change of heavy metal ions

$Bi^{3+} \rightarrow Bi^{2+} \rightarrow Bi^{+}(Bi)$

***J. Mat. Chem.* 19(2009)4603.**

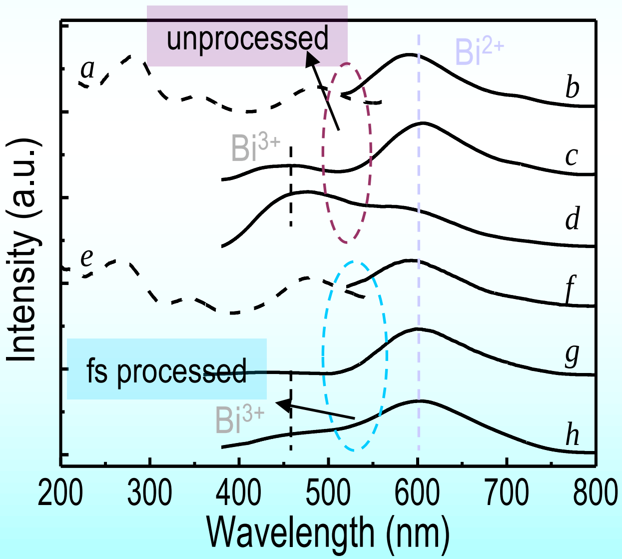

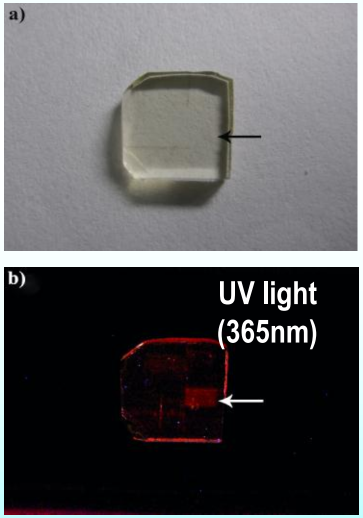

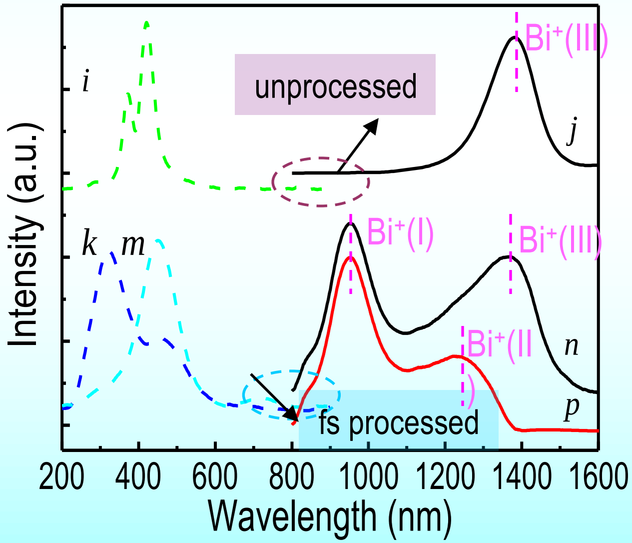

Visible and infrared luminescence changes after fs laser irradiation

Fs laser induced valence change of rare earth ions

$Eu^{3+} \rightarrow Eu^{2+}$ *Appl. Phys. Lett.*, 74(1999)10. **$Sm^{3+} \rightarrow Sm^{2+}$**

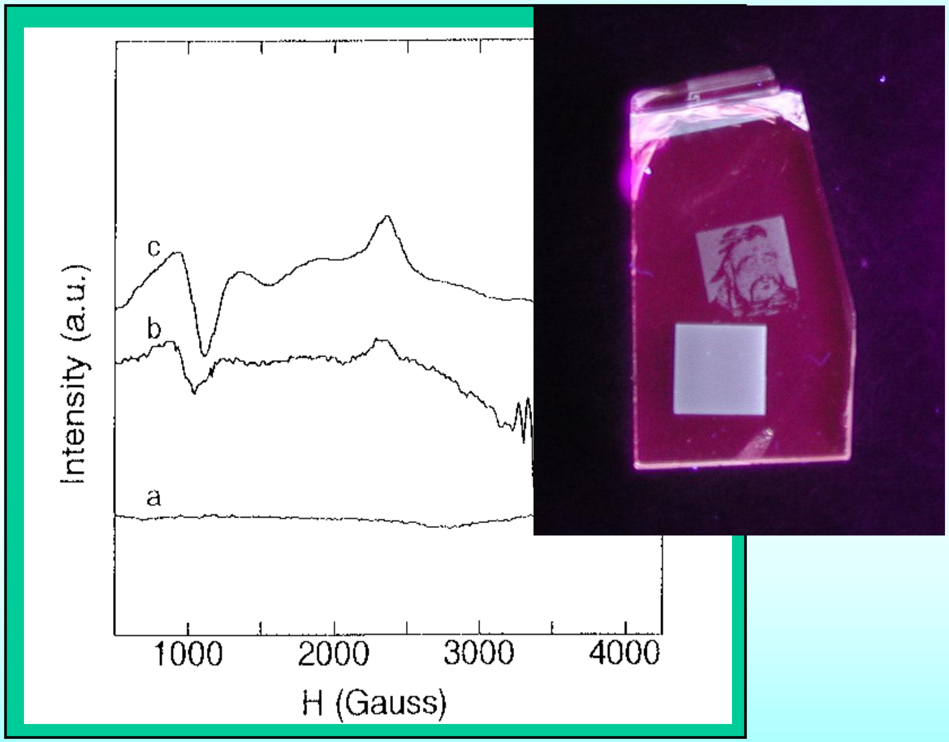

ESR spectra of Eu^{3+}-doped ZBLAN glass before (a) and after (b) the femtosecond laser irradiation and the spectrum (c) of a Eu^{2+} -doped AlF_3-based glass sample

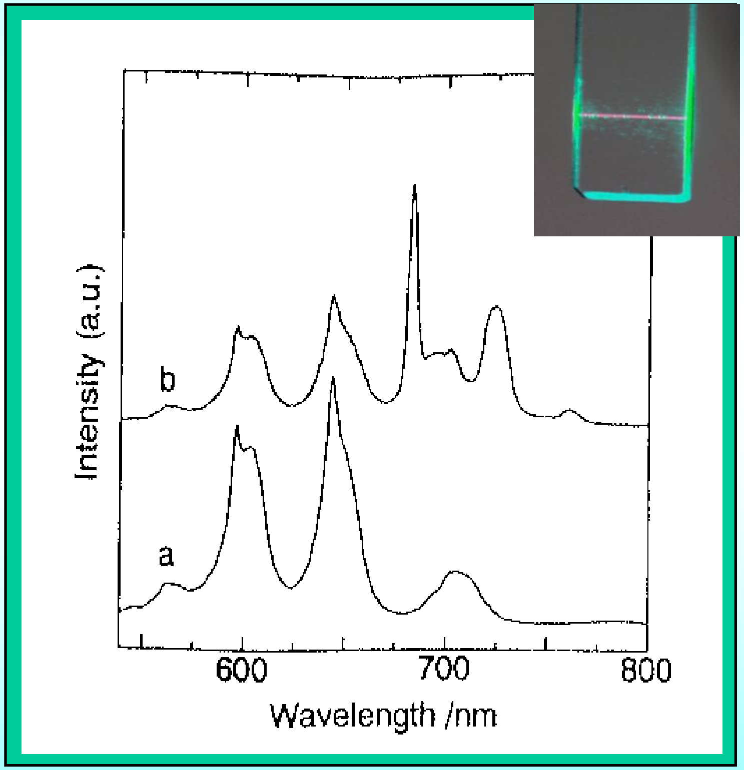

Potoluminescence spectra of a Sm^{3+}-doped borate glass before and after the femtosecond laser irradiation

3D rewriteable memory using valence state change of Sm ion

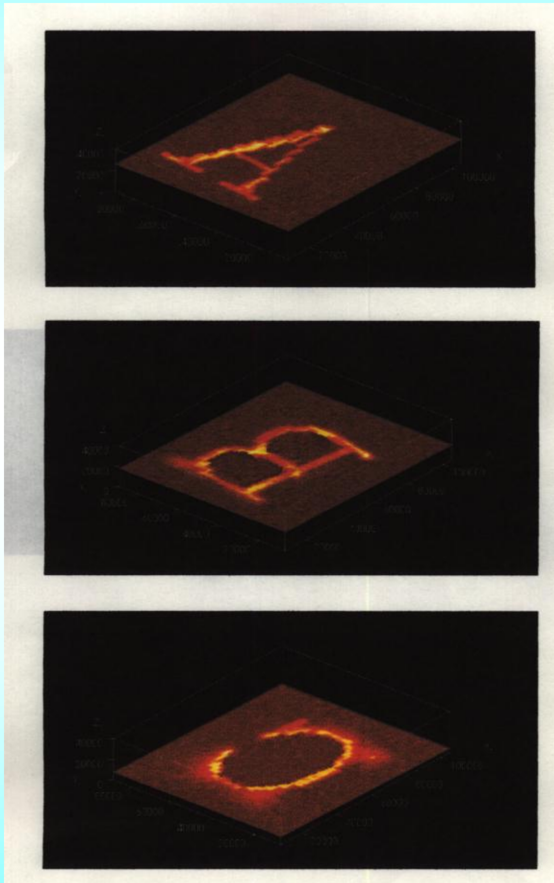

Three layers spaced 2μm

Appl. Phys. Lett., 80(2002)2263.

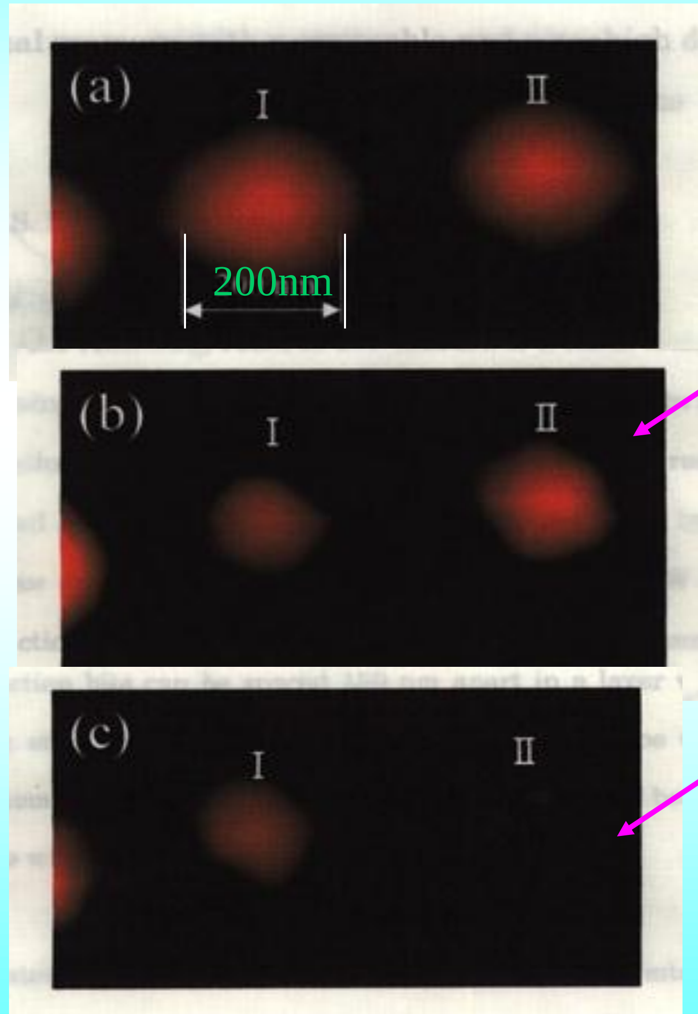

4f-4f Sm^{2+}
692nm

fs
488nm Ar^{+}

fs + 514nmAr^{+}
488nm Ar^{+}

Fs laser direct writing of refractive index changed pattern

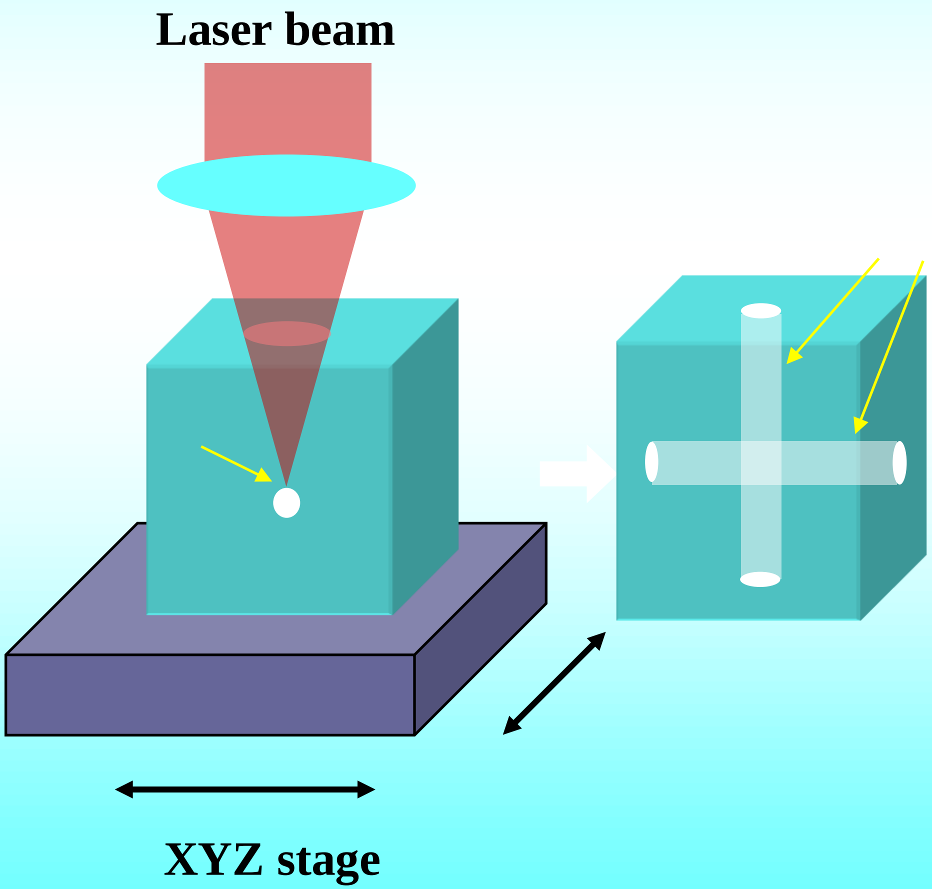

Direct writing of optical waveguide

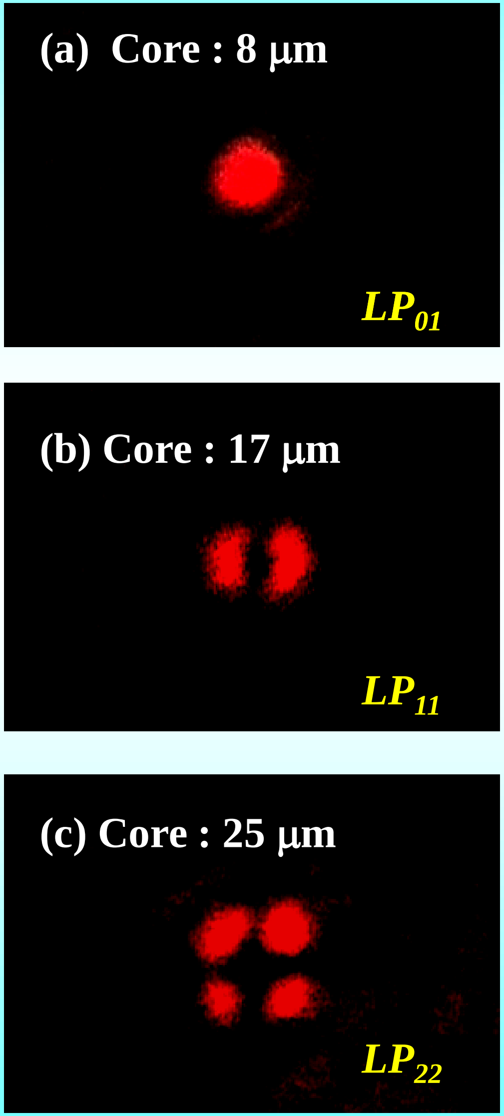

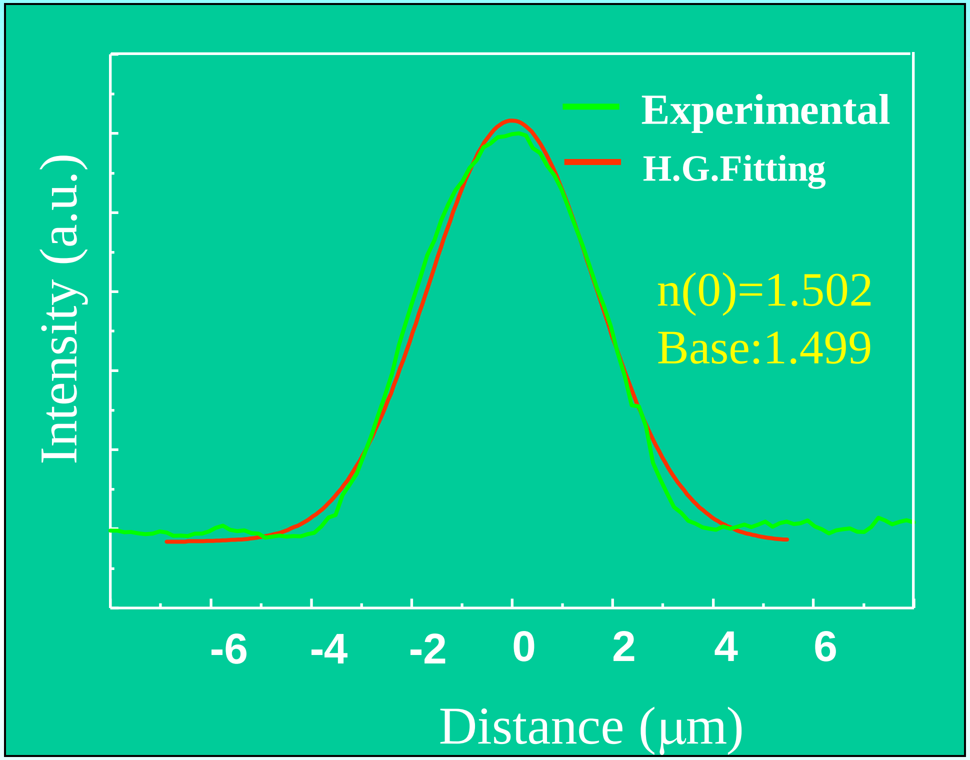

Result of Hermite-Gaussian fitting for the intensity distributions of the near field. The sample was the same as that observed in (a).The calculated result is almost in agreement with the experimental data, indicating that this waveguide is a graded-index type with a quadratic refractive-index distribution.

***Appl. Phys. Lett.*, 71(1997)3329.**

Direct writing of optical waveguide

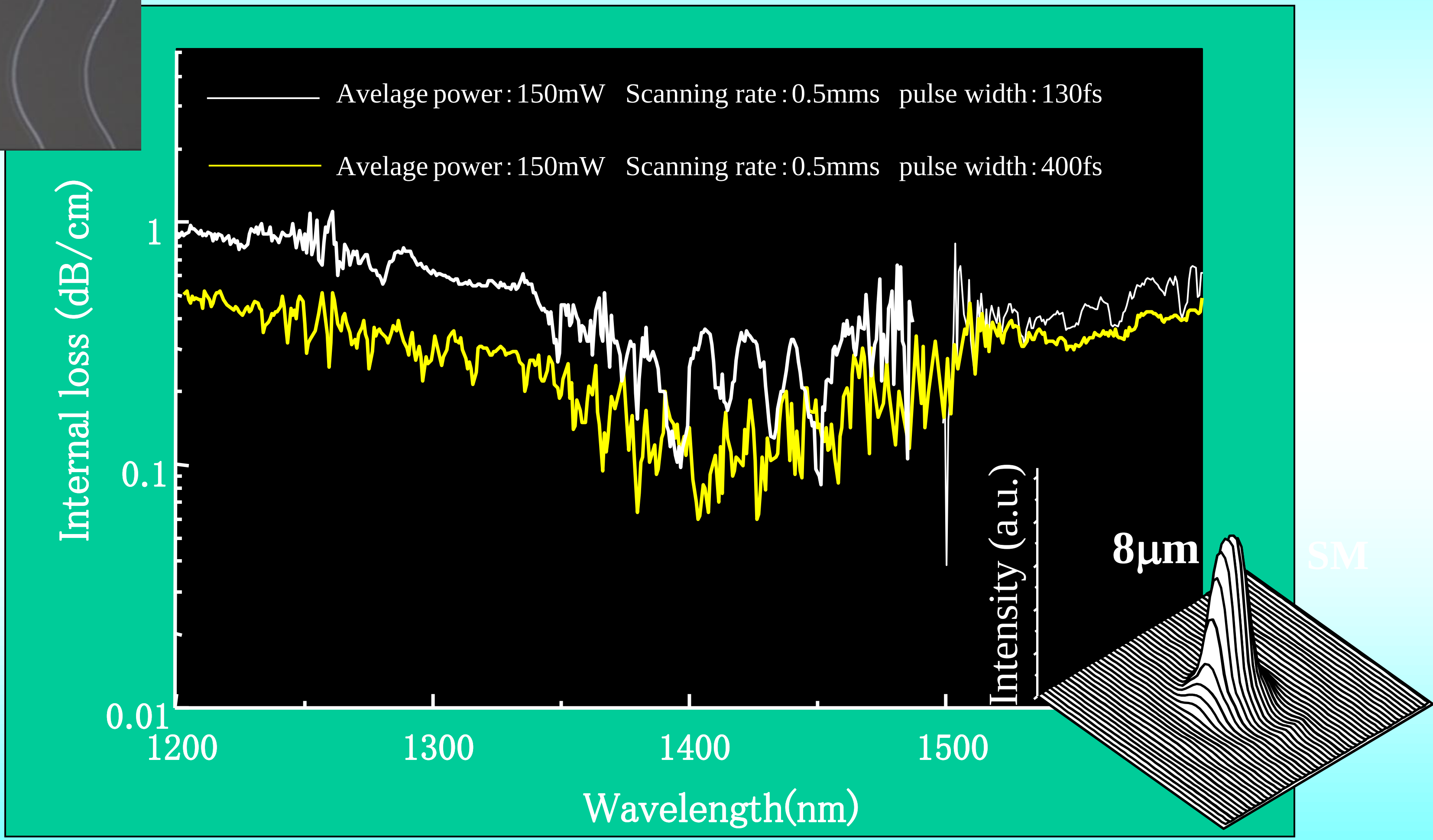

Internal loss of waveguides

Direct writing of grating and lens

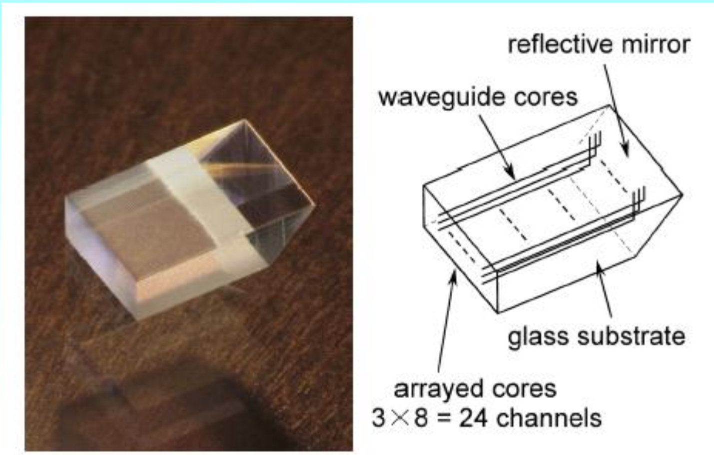

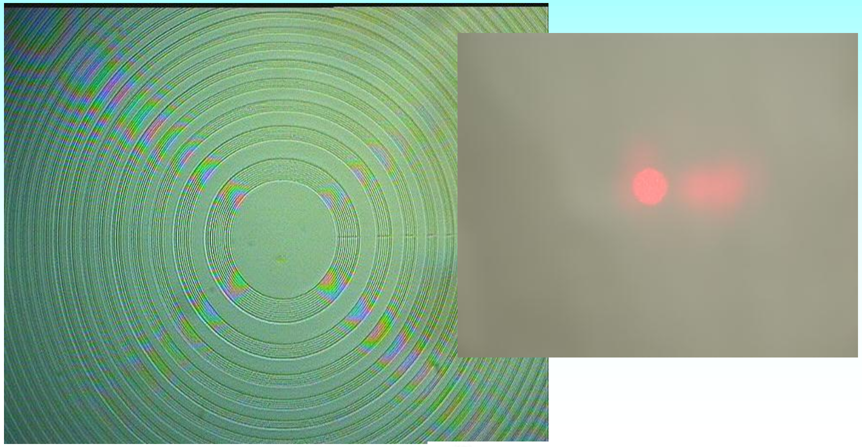

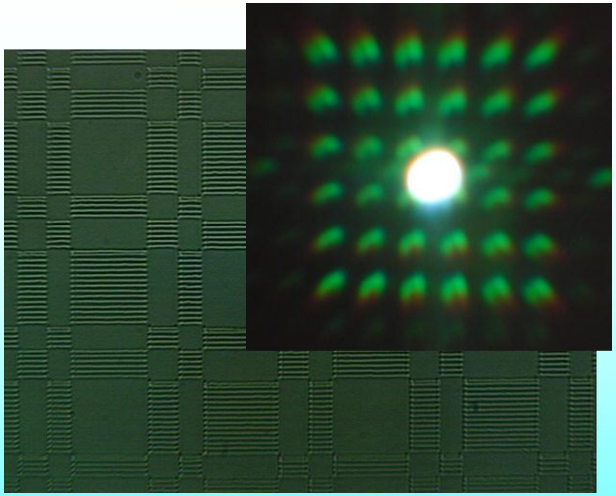

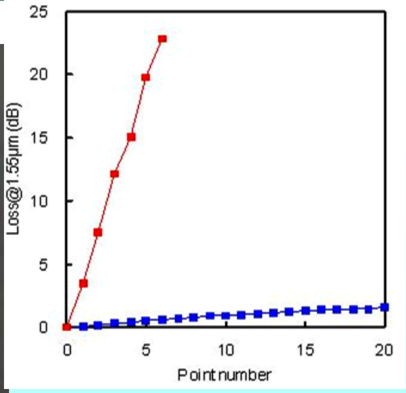

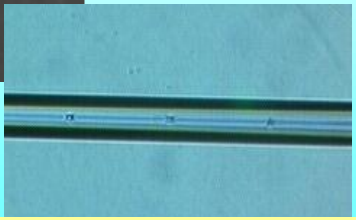

Appl. Phys. Lett., 71(1997)3329.

Opt. Lett., 29(2004)2728.

Direct writing of integrated DOEs

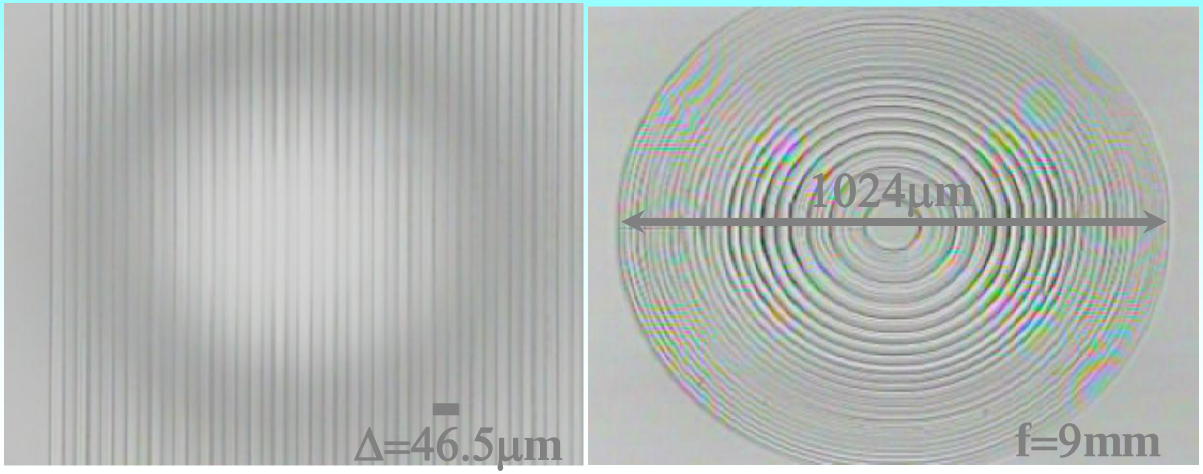

Grating & Binary lens (microscopic view)

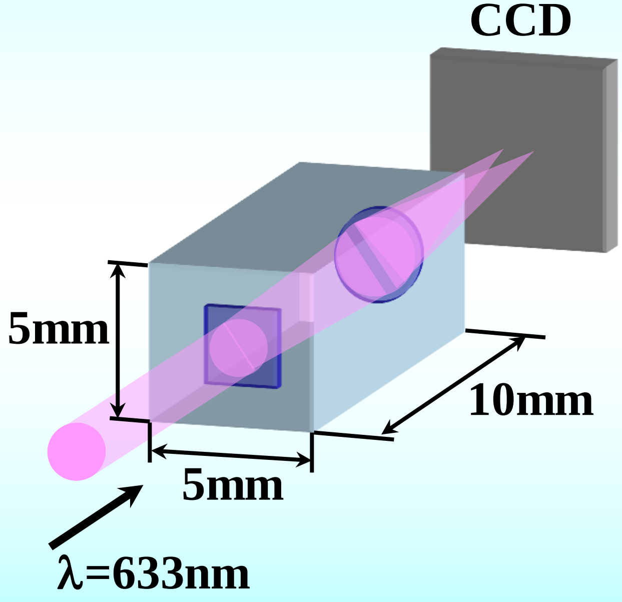

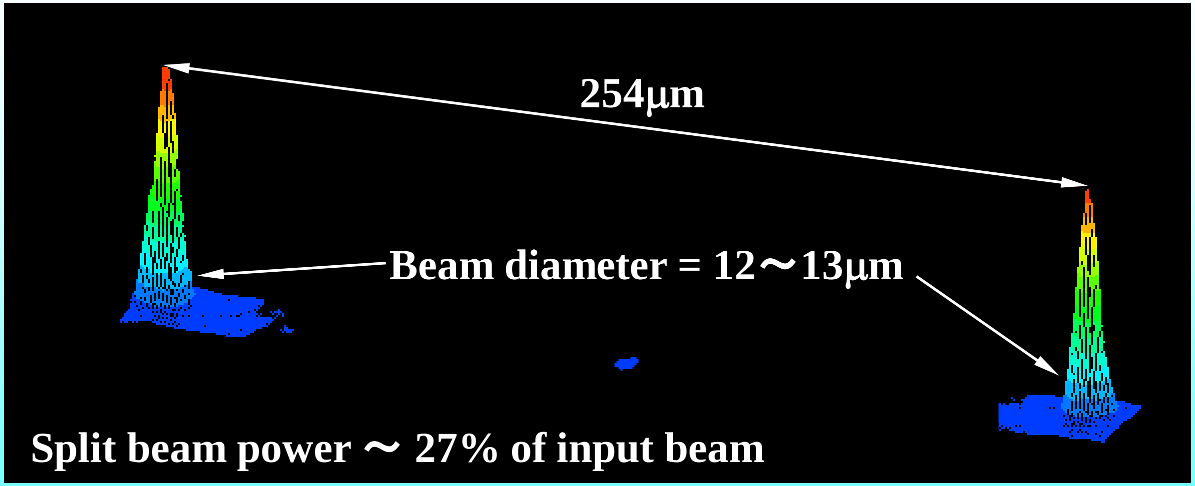

Beam profile at the focal plane

Direct writing of optical waveguide

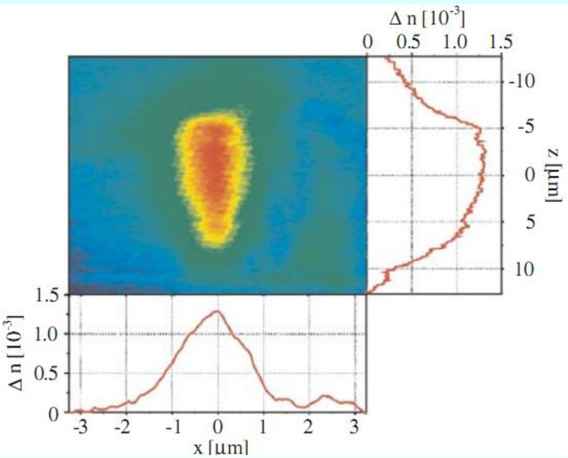

Single line type

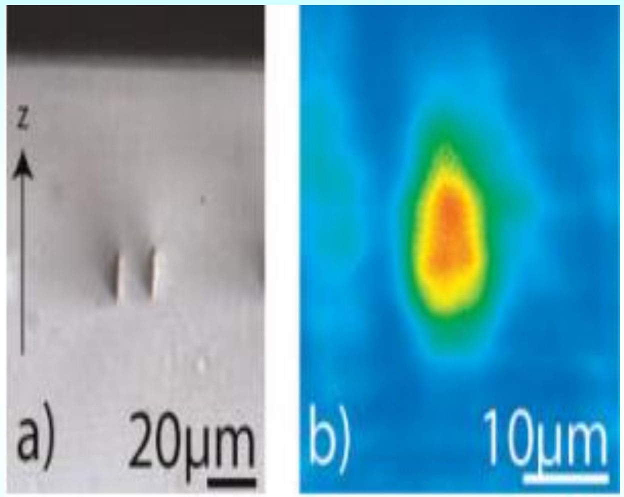

Double line type

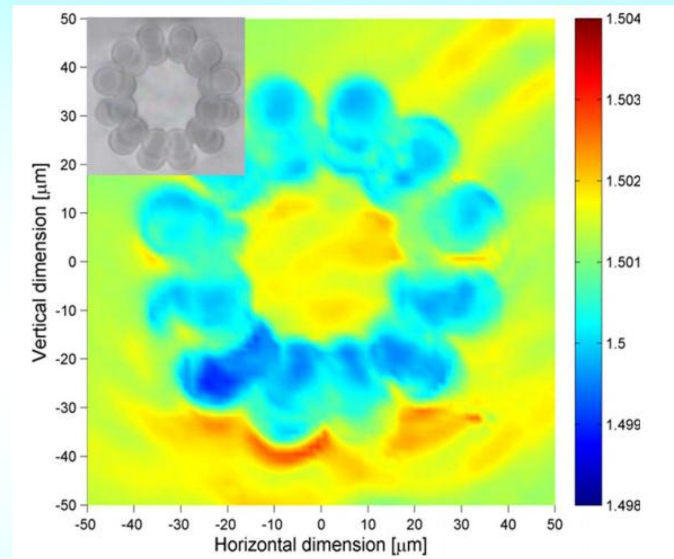

Circular type

Jens Thomas,et al, *Phys Status Solidi A 208*(2), 276-283(2011).

D.G.Lancaster, et al. *Optics Letters*, 36(9), 1587-9(2011).

Precipitation of functional crystal

SHG crystals ($Ba_2TiSi_2O_8$)

***Opt. Lett.*, 25(2000)408.**

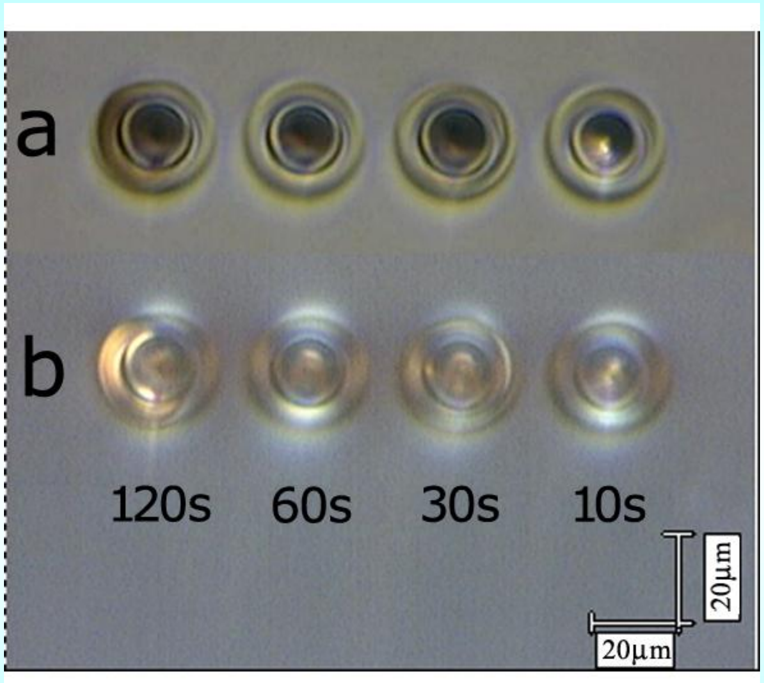

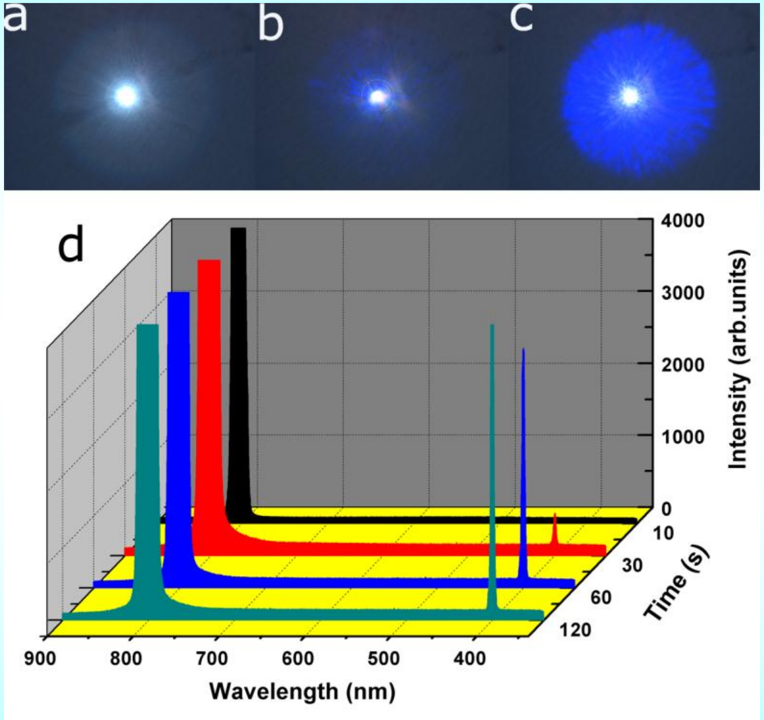

Microphotographs of the focal regions under the glass surface of 200mm illuminated by a) the natural light and b) the cross-polarized light after fs laser irradiating for 10s, 30s, 60s and 120s, respectively.

Photographs around the focal regions during fs laser irradiating for (a) 10s, (b) 30s, (c) 60s, respectively. (d) Time dependence of second-harmonic intensity during fs laser irradiation.

Space-selective precipitation of crystals

TiO_2 crystals

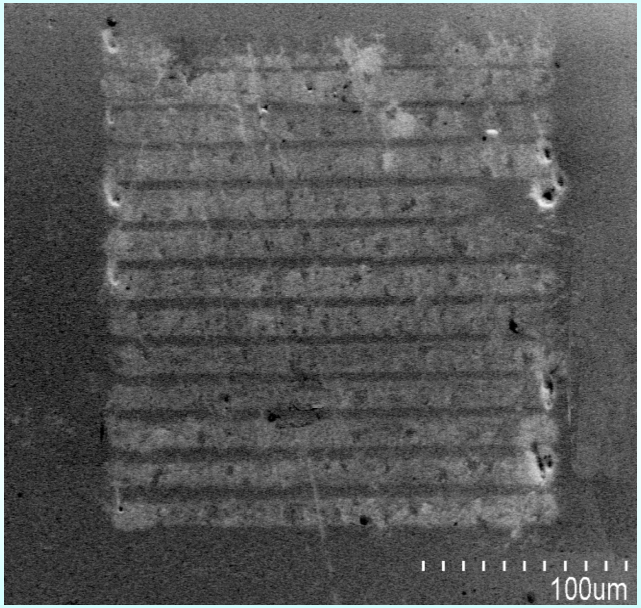

Microphotograph of the fs laser irradiated TiO_2-B_2O_3-SiO_2 glass.

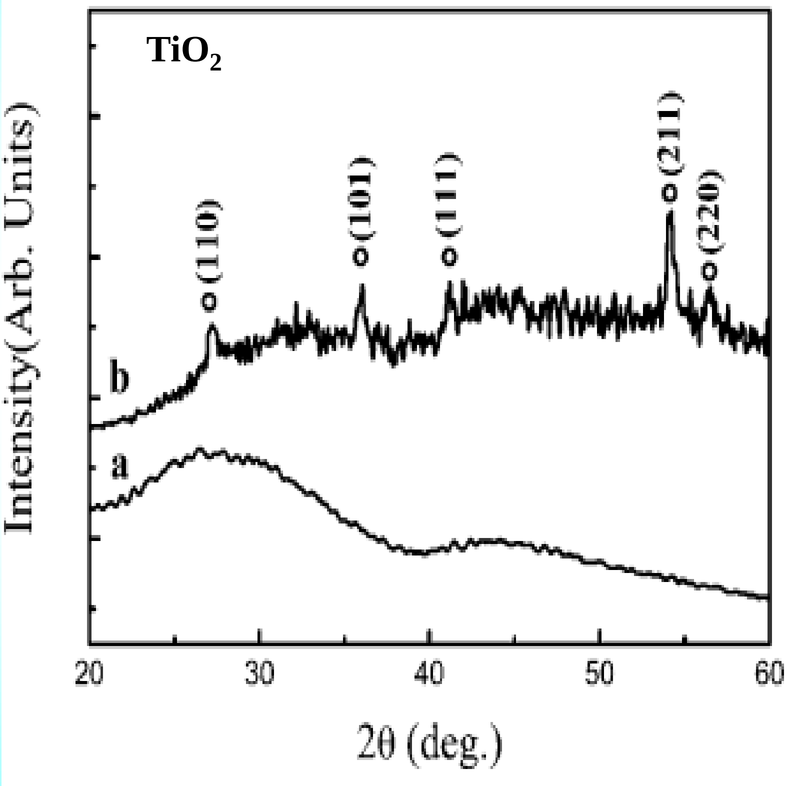

XRD pattern of the glass before and after the laser irradiation.

Space-selective precipitation of crystals

Yb^{3+}-Er^{3+} co-doped CaF_2 nanocrystals

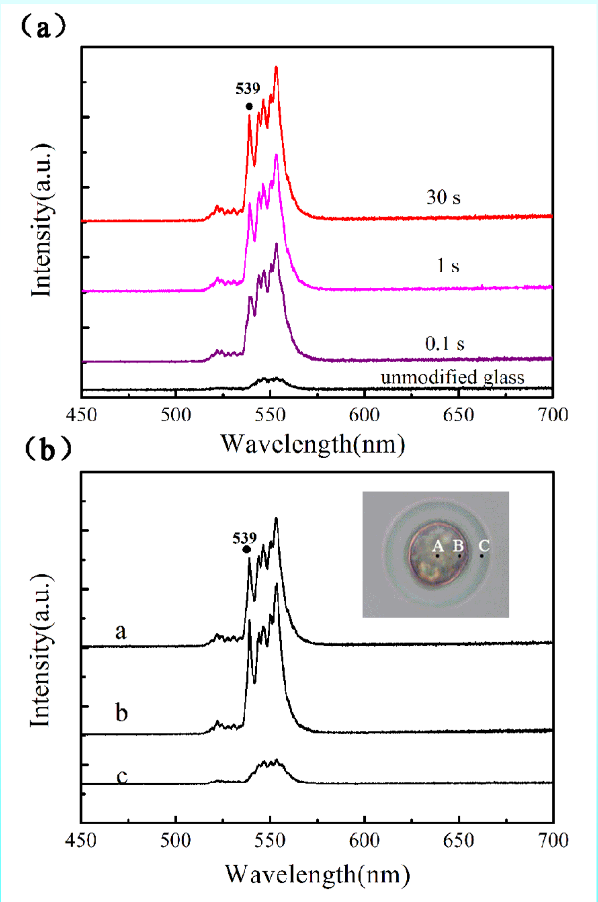

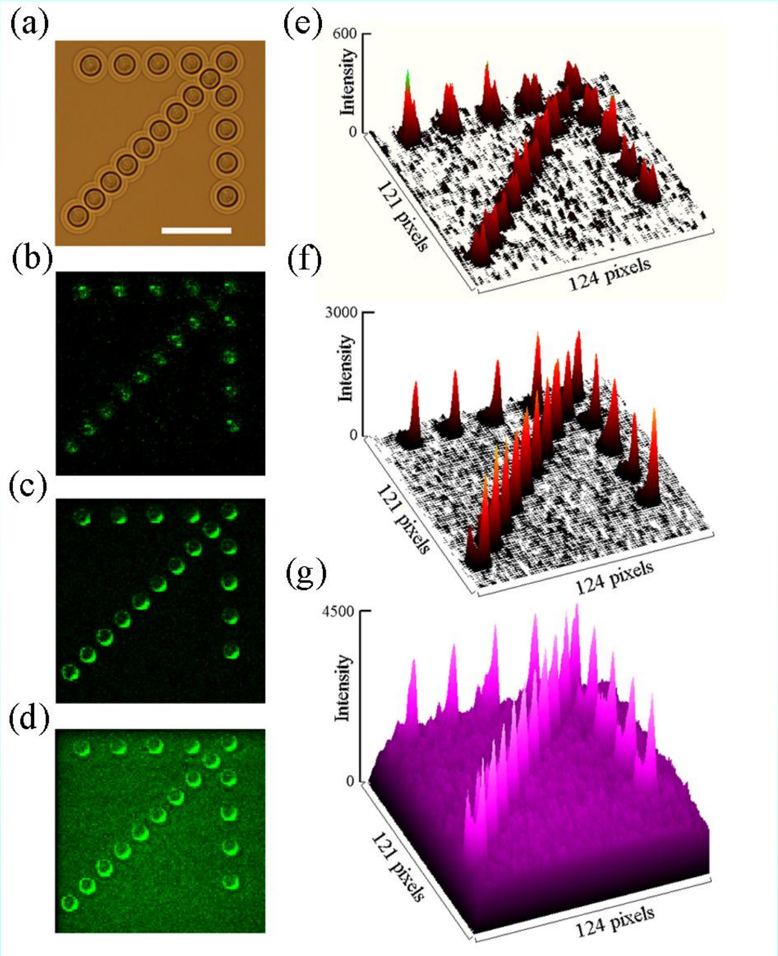

Space-selective precipitation of nanoparticles

Metal: Au, Ag, Cu, Pb, Zn, Ga, Na etc.

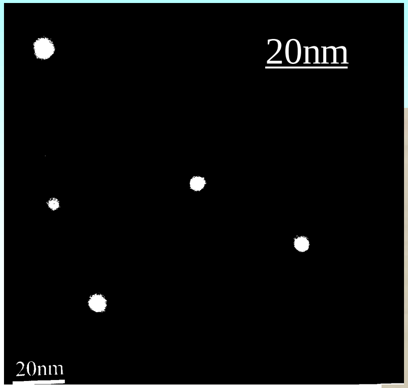

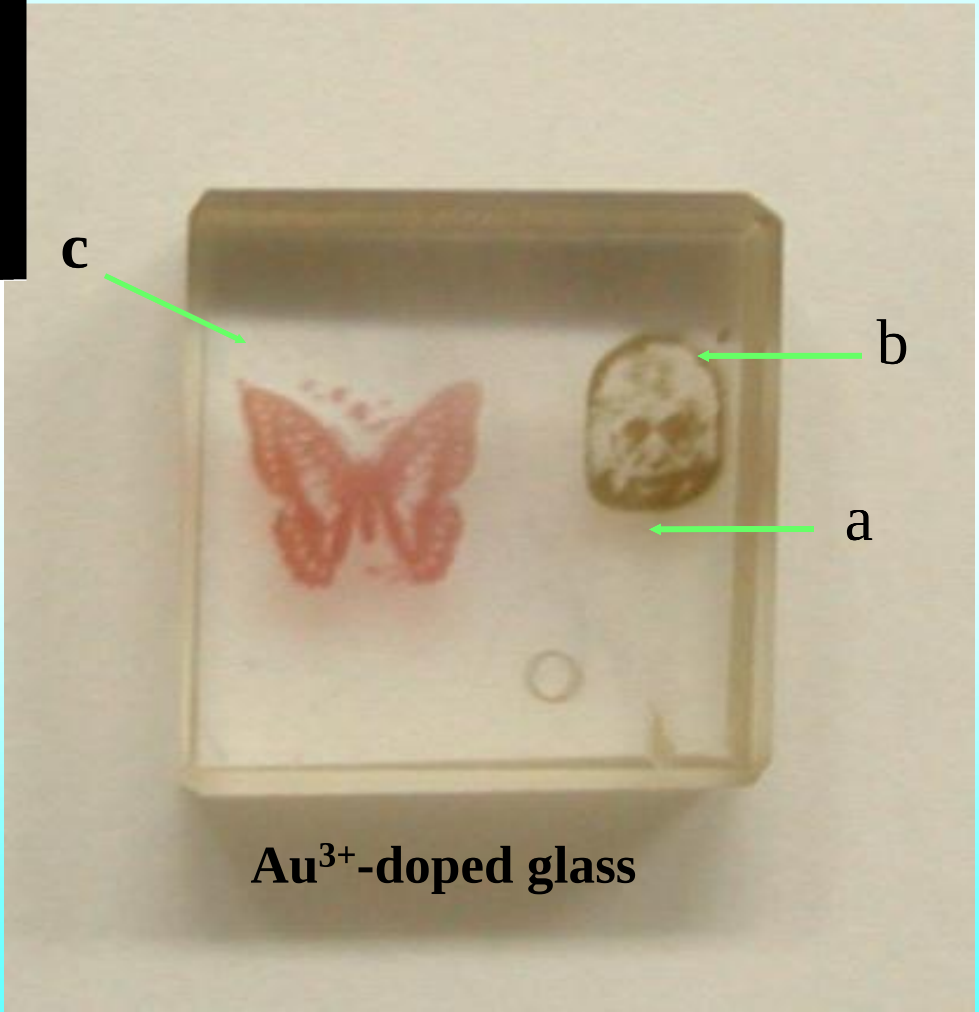

Au^{3+}-doped glass

a:before irradiation

b:after irradiation

c: after annealing at 550℃ for 10min

***Angew. Chem. Int. Ed.*, 43(2004)2230.**

Size control of precipitated Au nanoparticles

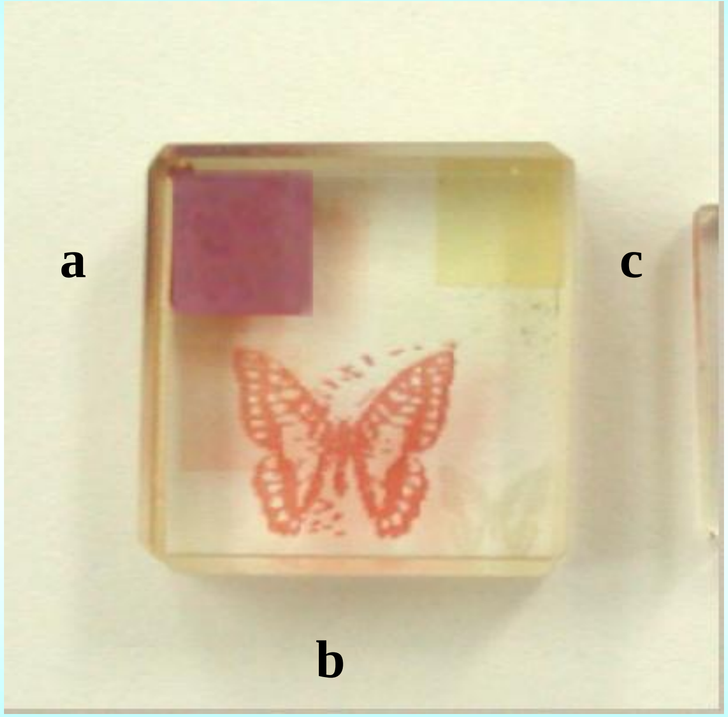

a: 6.5 x 10^{13}W/cm^2
b: 2.3 x 10^{14}
c: 5.0 x 10^{16}

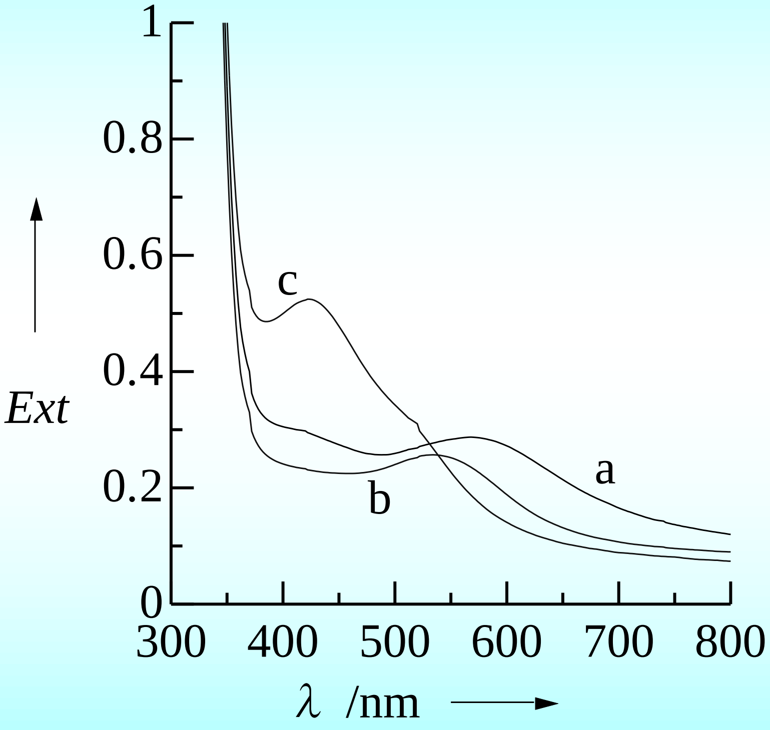

Absorption spectra

***Angew. Chem. Int. Ed.*, 43(2004)2230.**

Space-selective dissolution of Au nanoparticles

***Angew. Chem. Int. Ed.*, 43(2004)2230.**

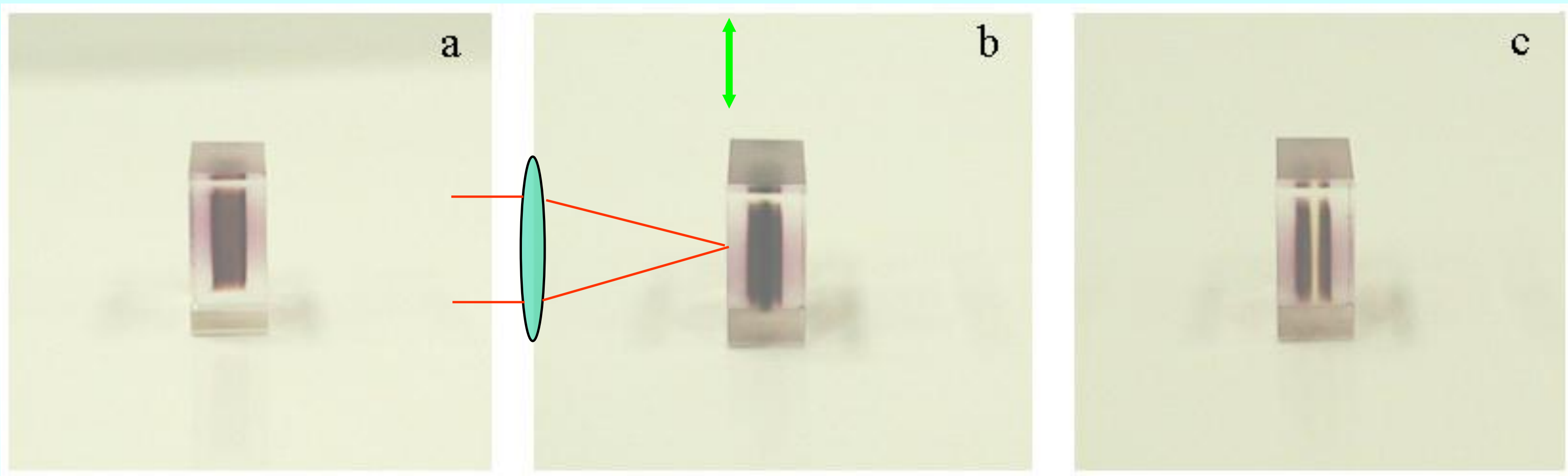

a: before second laser irradiation

b: after second laser irradiation

c: after second laser irradiation and annealing at 300℃ for 30min

Three-dimensional engrave in glass

Space-selective precipitation of nanoparticles

Semiconductor: Si, Ge, PbS, PbSe etc.

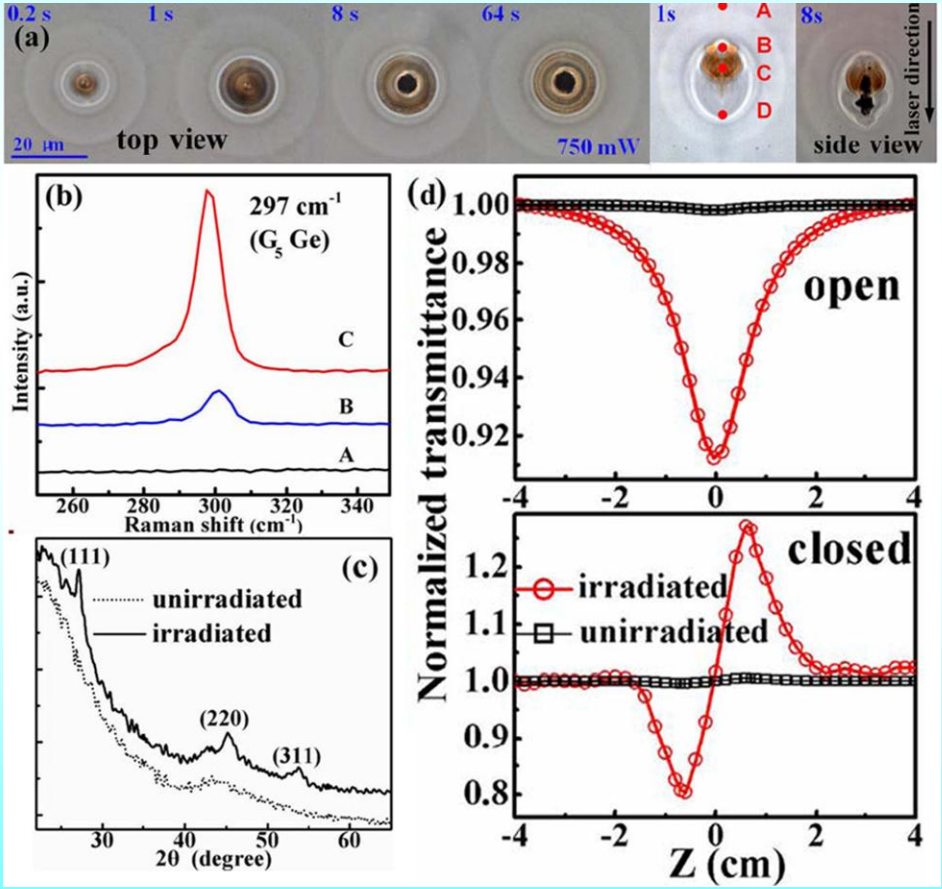

a: Optical microscope images

b: Raman spectra

c: XRD patterns

d: Z-scan results

***Opt. Lett.*, 92(2011)1211.**

AFM observation of micro-grating in glasses by interference field of ultrashort pulsed lasers

(ω+ω)

Appl. Phys. Lett., 80(2002)359.

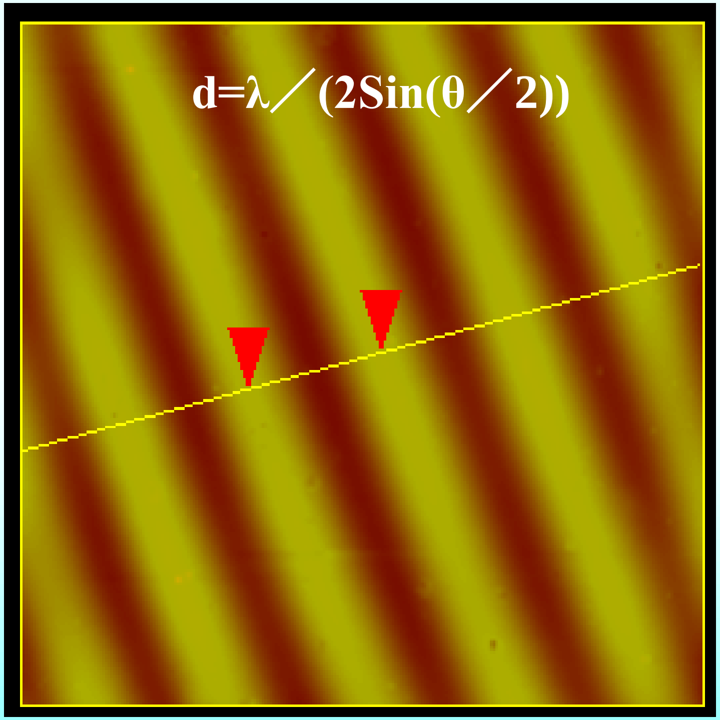

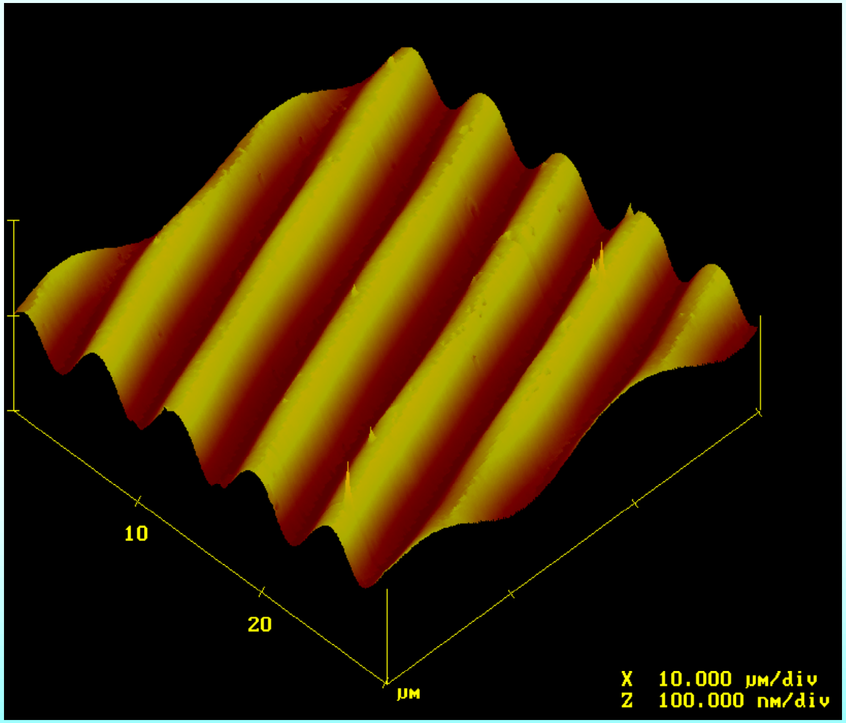

η＞90%

Observation of micro-grating in azobenzene polyimide by interference field of ultrashort pulsed lasers

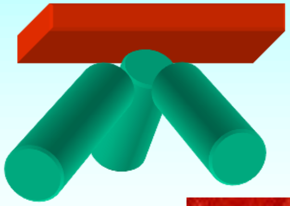

(ω+ω+ω)

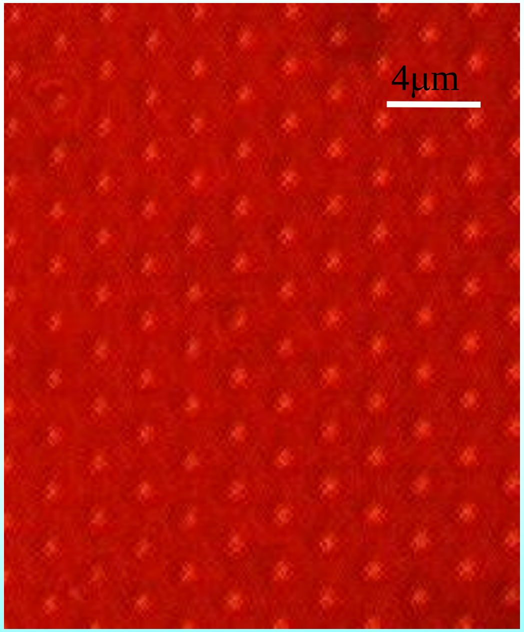

$\theta = 7°$
d = 4 μm

$\theta = 15°$
d = 2 μm

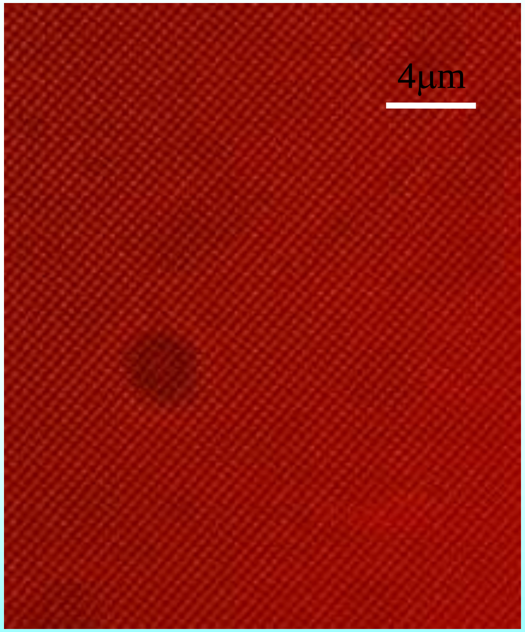

$\theta = 45°$
d = 0.7 μm

Microstructures by interference field of ultrashort lasers

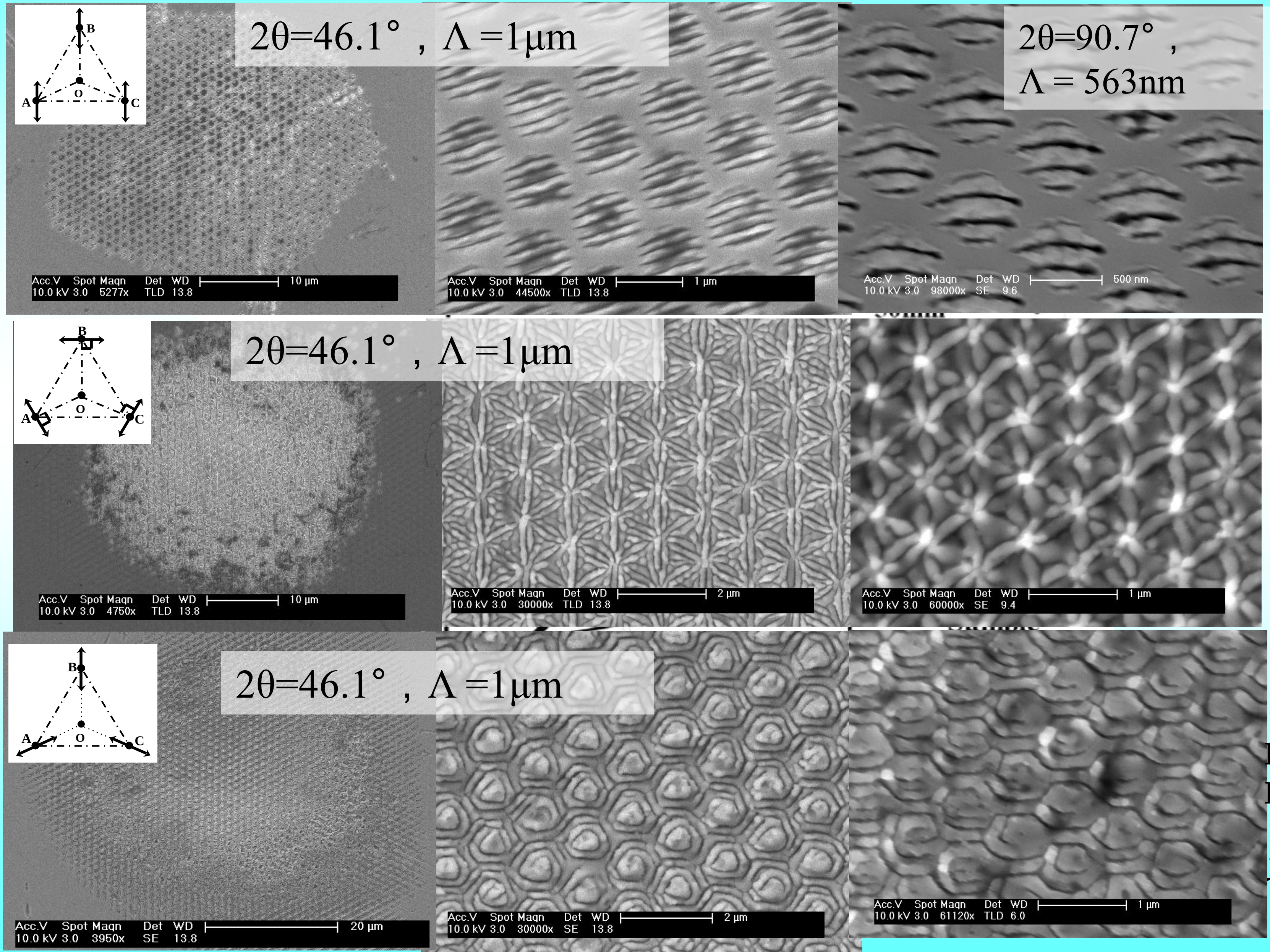

ZnO

Polarization Direction

uctures

All-optical poling (ω+2 ω)

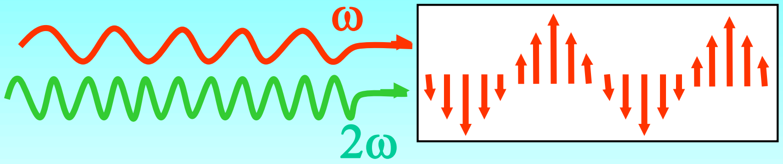

Photoinduced noncentrosymmetry $\chi^{(2)}$

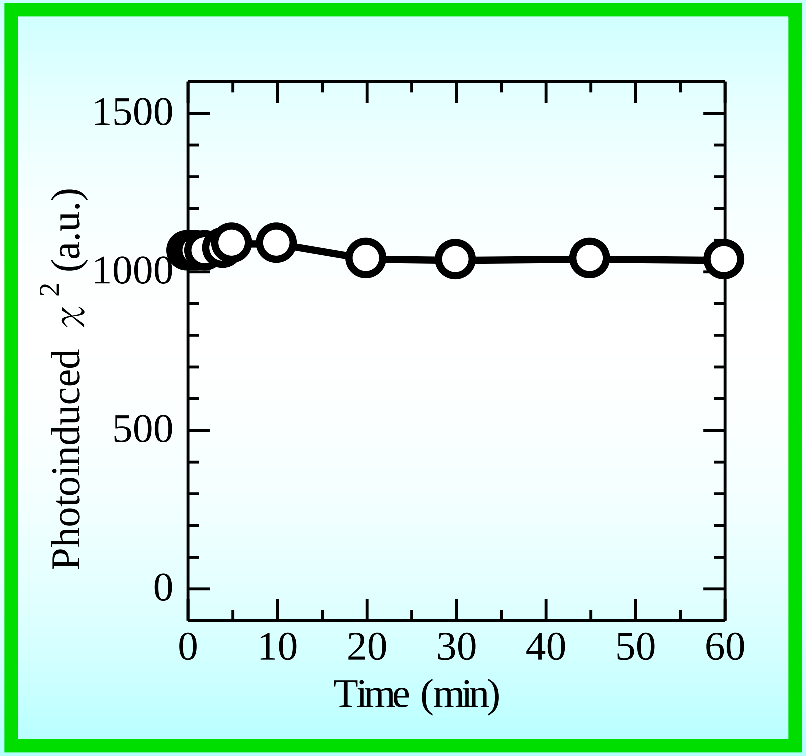

***Opt. Lett.*, 26(2001)914**

.

Non-linear interference field induced large and stable second harmonic generation in chalcogenide glasses.

Features of femtosecond laser

1fs=10^{-15}s

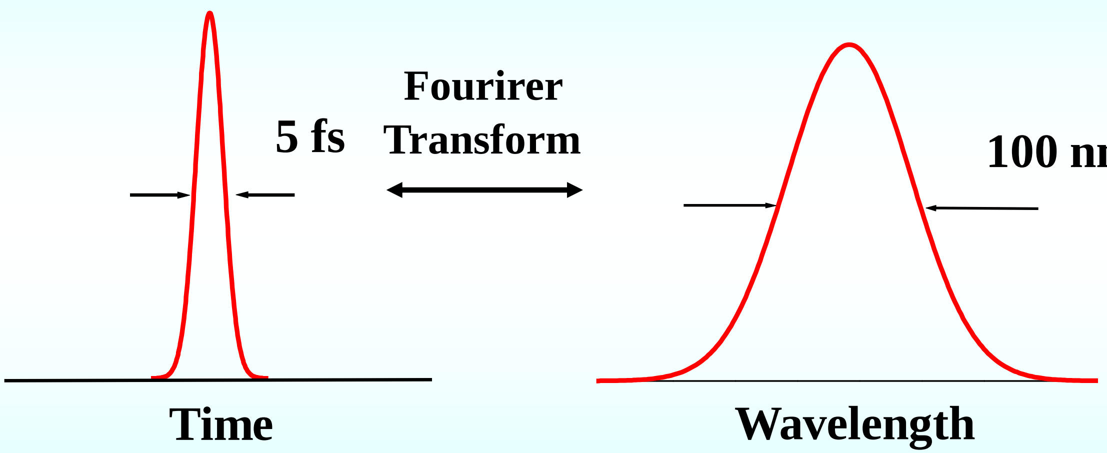

1) ultrashort pulse

2) ultrahigh electric field (>$2x10^{16}$W/cm^2)

3) ultrabroad bandwidth (coherent) ($\Delta \nu = k / \Delta \tau$)

Pulse-shaping: Spatial Mask

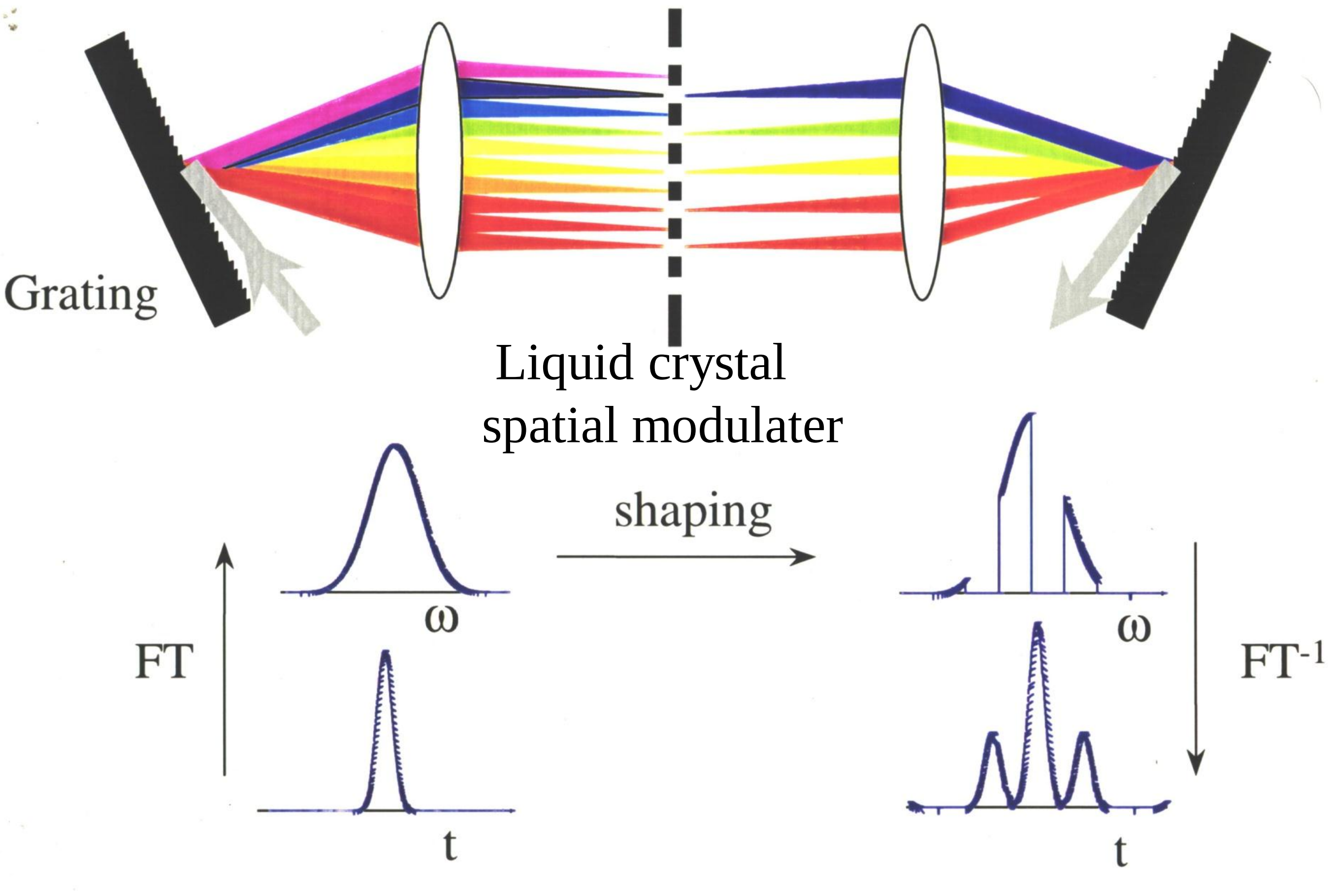

Various mysterious emission patterns

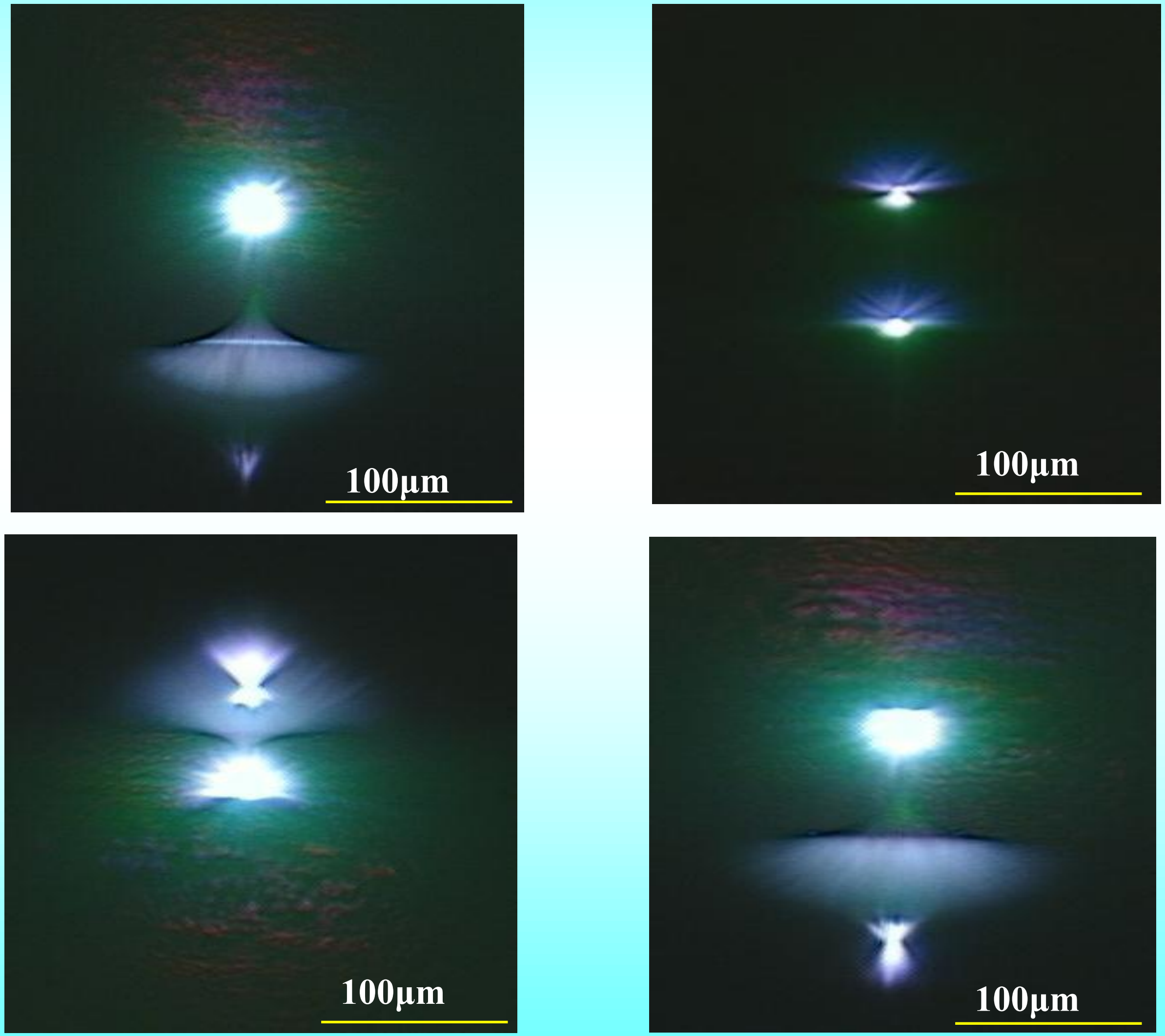

Conclusion

We have observed many interesting phenomena due to the interaction between femtosecond laser and transparent materials e.g. glasses.

We have demonstrated 3D rewritable optical memory, fabrication of 3D optical circuits, 3D micro-hole drilling, and 3D precipitation of functional crystals.

Our findings will pave the way for the fabrication of functional micro-optical elements and integrated optical circuits.

Grazie ！

谢谢! Thanks！ありがとう！

Merci ！ Danken ！ :Gracias ！

благодарю ！ Obrigado ！

당신을 감사하십시오 ！

qjr@zju.edu.cn